Computers and Electronics in Agriculture 237 (2025) 110480

Contents lists available at ScienceDirect

Computers and Electronics in Agriculture

journal homepage: www.elsevier.com/locate/compag

Review article

Identification and analysis of key factors limiting the performance of electrical soil sensors: A review

Anthony Alhadchiti [a,b,*], Bojan Nikolic [a,b], Panagiotis Ioakim [b], Michael B. Powner [c], Iasonas F. Triantis [a]

[a] Research Centre for Biomedical Engineering, School of Science and Technology, City St George's, University of London, London, ECIV 0HB, UK
[b] Delta-T Devices Ltd, Burwell, Cambridge, CB25 0EJ, UK
[c] Centre for Applied Vision Research, School of Health and Medical Sciences, City St George's, University of London, London, ECIV 0HB, UK

ARTICLE INFO

Keywords:
Amplitude domain reflectometry
Broadband dielectric spectroscopy
Capacitance
Electrical conductivity
Fertilisers
Frequency domain reflectometry
Impedance
Moisture
Resistance
Soil sensor
Temperature
Time domain reflectometry
Water tension

ABSTRACT

Current agricultural practices are increasingly adopting sustainable methods to achieve high crop yields and meet market demands. However, the excessive use of water and fertilisers has led to issues such as food insecurity and climate change. The over-application of plant nutrients increases food prices and results in unused fertilisers contributing to harmful greenhouse gas emissions, which affect the ozone layer. This raises the question: why are excessive amounts of water and fertiliser wasted despite the availability of agricultural sensors and technologies that aim to improve sustainability? This paper critically examines the underlying theory and technology behind these practices to identify their challenges and limitations. The review focuses on the shortcomings of current soil theories, covering soil physics, electrical properties, and factors influencing soil characteristics. Additionally, this paper discusses various techniques used to measure the electrical properties of soil, including traditional methods, capacitive sensors, time-domain and frequency-domain reflectometry, amplitude-domain reflectometry, and broadband dielectric spectroscopy. The challenges and limitations of these techniques are also explored. Furthermore, the paper addresses the theory and challenges of electrical property measurement techniques at the system level, analysing the injection, load, and output stages to identify the difficulties in each part.

Contents

1. Introduction 2
1.1. Review methodology 3
2. Theoretical analysis of soil electrical properties 3
2.1. Soil electrical properties 3
2.2. Factors influencing soil characteristics 4
2.3. Limitations of soil theory 7
3. Measurement of soil electrical properties 8
3.1. Measurement techniques 8
3.1.1. Traditional measurement techniques 8
3.1.2. Capacitive sensors 8
3.1.3. Time domain reflectometry 9
3.1.4. Frequency domain reflectometry 10
3.1.5. Amplitude domain reflectometry 11
3.1.6. Broadband dielectric spectroscopy 11
3.2. Challenges and limitations of measurement techniques 12
3.3. Theory and challenges of the electrical properties measuring techniques at system level 13
3.3.1. Injection stage measuring technique 13

* Corresponding author at: Research Centre for Biomedical Engineering, School of Science and Technology, City St George's, University of London, London, ECIV 0HB, UK.
E-mail addresses: anthony.alhadchiti@city.ac.uk (A. Alhadchiti), bojan.nikolic@delta-t.co.uk (B. Nikolic), panos.ioakim@delta-t.co.uk (P. Ioakim), michael.powner@city.ac.uk (M.B. Powner), i.triantis@city.ac.uk (I.F. Triantis).

https://doi.org/10.1016/j.compag.2025.110480
Received 25 November 2024; Received in revised form 8 April 2025; Accepted 28 April 2025
Available online 14 May 2025

3.3.2. Load stage measuring technique 14
3.3.3. Output stage measuring technique 16
4. Conclusion 17
CRediT authorship contribution statement 17
Declaration of competing interest 17
Acknowledgements 17
Data availability 17
References 17

1. Introduction

In the face of increasing food insecurity and the intensifying effects of global climate change, addressing the unsustainable practices in agriculture, particularly concerning water and fertiliser management, is imperative. Agriculture stands as a significant contributor to global water consumption, utilising up to 90% of the world's freshwater resources. However, inefficiencies in irrigation methods contribute to substantial water wastage, with approximately 50% of water used in agriculture being lost due to ineffective practices (Menne et al., 2021; Ahmed et al., 2022). The implications of these practices are profound, contributing to food insecurity and compounding environmental strain amidst changing climatic conditions. Moreover, they impose significant negative financial impacts, amplifying the economic burden on agricultural sectors worldwide.

To combat these inefficiencies, the integration of advanced sensor technologies in agricultural practices has become crucial. Sensors play a pivotal role in optimising water and fertiliser usage, thereby enhancing the sustainability of agricultural practices. By providing real-time data on soil moisture levels, nutrient content, and crop health, sensors enable precise and targeted application of water and fertilisers. This not only minimises waste but also ensures that crops receive the exact amount of resources they need for optimal growth, leading to improved yields and reduced environmental impact.

Fertilisers, nitrogen specifically, play a critical role in boosting crop yield and ensuring food security globally. However, large inputs of such fertilisers to croplands result in increased adverse environmental impact and pose a threat to human health (Quan et al., 2021). Inadequate use of fertilisers, for instance placing fertilisers away from the roots of the plant or in an inopportune moment of the plant's growth cycle, leads to the loss of fertilisers through leaching or conversion into a harmful gas (Duncombe, 2021). Consequently, the use of fertilisers should be monitored knowing that the nitrogen use efficiency is 46% globally (Zhang et al., 2021).

Soil moisture, water matric potential, fertigation, temperature, pH, metals, texture, and living organisms all play a role in influencing and describing the properties of the soil. Soil moisture is the amount of water contained in the soil (Kumar et al., 2016). Soil matric potential refers to the tension exerted by the soil to retain water, which limits the amount of water that plants can draw from the soil with their roots (Menne et al., 2021). Fertigation is the act of applying fertilisers, such as nitrogen (N), phosphorus (P), and potassium (K), to optimise nutrient delivery to crops (Siontorou and Georgopoulos, 2016). The above-mentioned soil properties can be monitored by using different methods of sensing, such as chemical, optical, or electrical sensors, which will be covered in the following paragraphs.

Chemical sensors, such as ion-sensitive field effect transistors (ISFET) or chemiresistors, are composed of selective materials surrounded by one or multiple pairs of electrodes (Zheng et al., 2023). When the selective sensitive film material encounters the target analytes, electron transfer and acquisition occurs on the film surface (Zheng et al., 2023). However, due to the degradation of selective membranes after a while, and the cross-sensitivity of different ions available in the soil, it is very difficult to assess the various concentrations of different ions contained in the soil (Ohkawara et al., 2022).

Optical sensors such as visible light, infrared, and fibre optic sensors, play a role in measuring soil properties. The concept of optical light sensors is based on the interaction between the soil surface properties and the incident light. Nitrogen, phosphorus, and potassium, (NPK) concentration levels in the soil are directly related to the measured reflected light detected by a photodiode since different amounts of RGB light absorption is caused by different NPK concentrations in soil (Fan et al., 2022). However, this type of optical sensor is not very accurate due to interference from the surrounding environment (limited visibility and susceptibility to weather conditions) and it does not convey any information about the in-depth soil characteristics (Fan et al., 2022; Abdulraheem et al., 2023).

Electrical sensors and technologies, for example, time-domain reflectometry (TDR), frequency-domain reflectometry (FDR), amplitude-domain reflectometry (ADR), capacitive, and impedemetric sensors, are being widely used in assessing the different soil properties (Da Costa Junior et al., 2021). In soil, ions are the charge carriers, so the movement of ions will lead to the movement of charges, therefore, the conductivity in soil is electrolytic (ionic) (Datsios and Mikropoulos, 2019). Soil's electrical conductivity correlates with the previously mentioned diverse physical and chemical properties. Considering the challenges encountered by chemical and optical sensors, along with the electrical measurability of soil characteristics, it can be concluded that the most suitable method for long-term soil monitoring involves sensing the soil's electrical properties, with the soil's electrical conductivity being one of the most important measurands.

Measuring the soil's electrical characteristics is also useful for different applications of engineering and science, such as geological surveys, remote sensing, soil contamination studies, grounding system design and analysis, and electromagnetic transient studies (Datsios and Mikropoulos, 2019).

However, despite a plethora of technologies and sensors being available to measure the electrical characteristics of the soil, their performance in measuring hydration and fertigation levels is lacking. Therefore, reviewing the performance and in situ applicability of the available methods and identifying their limitations is highly desirable.

Any soil sensor system comprises four different layers, namely, soil physics, sensing element, instrumentation or circuitry, and data processing. In this review, our focus will be on the first three layers (soil physics, sensing element, and circuitry). This review aims to present the latest methods used for measuring the electrical characteristics of soil and to examine the potential errors in these systems. The underlying theory behind these technologies will be discussed and reviewed. Then, the technical aspects, such as the operating principles of different soil electrical characteristics measuring techniques, will be critically analysed to understand and highlight the limitations of the available systems on the market.

While researchers and scientists commonly highlight the advantages and benefits of their conducted research and developed sensors, this focus often makes it challenging to address the disadvantages. However, in this paper, we aim to diverge from this trend by presenting a critical examination of the challenges and limitations inherent in the current theory and technology.

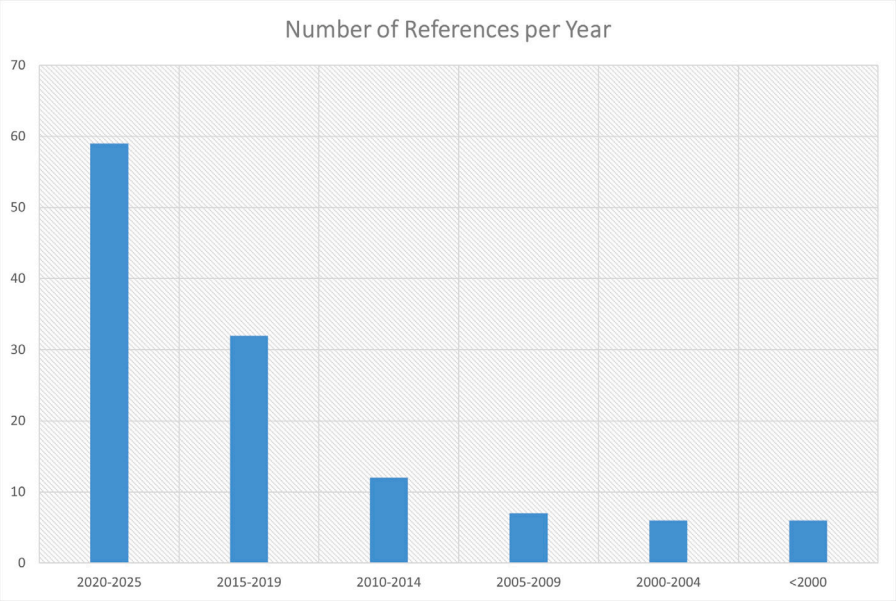

Fig. 1. Number of resources per year group.

1.1. Review methodology

To conduct this review paper, we focused on research topics mainly "electrical soil moisture sensor" and "electrical soil fertigation sensor". We primarily used google scholar and City St Georges University of London library in conducting our research to find articles that are published in different journals, mainly under Elsevier, IEEE, PubMed, Mdpi, and Springer. In addition to the mentioned keywords, we also researched the methods and techniques for measuring soil moisture and fertigations through non-electrical properties, such as optical and chemical methods. Our primary objective was to gather data from contemporary articles, as evidenced by the fact that the majority of our references have been published within the past five years. Nevertheless, the comprehensive nature of this review, which encompasses the theoretical foundations of the technology, necessitated the inclusion of older references to adequately address this aspect. More than 200 articles and reports have been read but only 122 references were been used in this review paper and these resources are distributed as listed in (Fig. 1).

2. Theoretical analysis of soil electrical properties

Soil in dry form is an insulating material with permittivity less than 10 (Datsios and Mikropoulos, 2019). Soil becomes a semi-conducting material when it gets wet; the permittivity of wet soil is notably higher than the permittivity of dry soil due to the presence of water because water has a high relative permittivity equivalent to 80.3 at 20 °C (Datsios and Mikropoulos, 2019; Hilhorst, 2000). Therefore, water content and its soil spatial distribution strongly affect the soil electrical properties (Datsios and Mikropoulos, 2019). In addition to soil moisture, other factors influence soil characteristics such as temperature, salinity, texture, organic matter content, inorganic matter content, porosity, and ion exchange capacity.

2.1. Soil electrical properties

Electromagnetic parameters (magnetic susceptibility, dielectric permittivity, and electrical conductivity) of the soil are related to the soil's chemical and physical properties (Spikic et al., 2022). Permittivity is a measure of the polarisation in a medium when subjected to an electromagnetic field (Xu et al., 2012). When insulators are exposed to an electric field, polarisation occurs (Xu et al., 2012). To understand

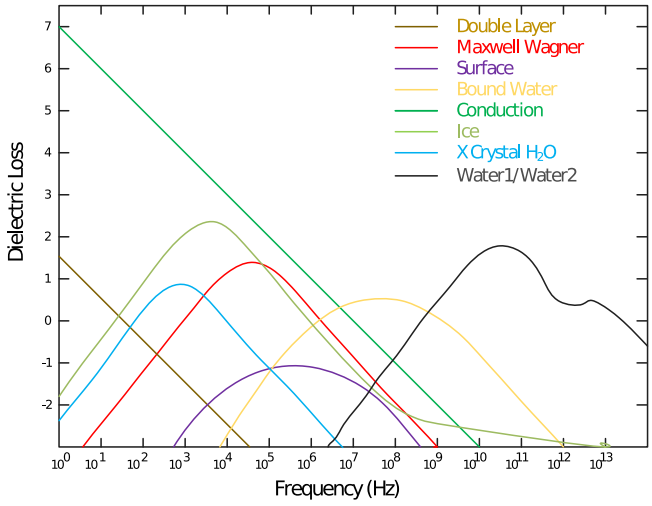

Fig. 2. Contributions of the imaginary part (ε'') of the relative permittivity of soil (dielectric loss) covering a large frequency spectrum. The mechanisms included in this figure are: conduction (ionic conductivity), double layer (charged), Maxwell-Wagner relaxation, conductivity of the surface, bound water or microscopically confined water relaxation. Water 1 represents the principle free water relaxation, and Water 2 is the second free water relaxation.
Source: Redrawn from González-Teruel et al. (2020).

the theoretical basis of material properties, we need to examine the properties of dielectric polarisation and relaxation. In our case, soil is a medium composed of multiple phases, consisting of different materials that exhibit various polarisation mechanisms (ionic, electrical, and orientational) (Xu et al., 2012). These mechanisms include the Maxwell-Wagner relaxation in the kHz range, bound-water relaxation in the MHz range, and free-water relaxation in the GHz range. These mechanisms are related to the types of interactions between water and soil particles (Zambrano et al., 2007). Fig. 2 illustrates the relationship between dielectric loss mechanisms in the soil at different frequencies (Ma et al., 2023).

As it can be seen from Fig. 2, multiple effects contribute to the complex dielectric constant. The double layer contributes to the dielectric loss at low frequencies. This is because at lower frequencies the

electric field changes direction slowly allowing the ions in the water molecules and the charged double layer to interact and respond with the field (Hillel, 1981). This phenomenon leads to higher dielectric loss at lower frequencies and it is absent at higher frequencies (Hillel, 1981). Another mechanism observed in Fig. 2 is the Maxwell-Wagner relaxation effect. This effect is also observed at low frequencies (typically less than 100 MHz). It arises mainly due to the heterogeneous nature of the soil (water, air, and solid particles) and the interface between the different elements in the soil (Revil et al., 2016). So when applying an AC signal into the soil, the different conductivities of the different available elements will build up charges at the interface acting like a mini-capacitor and limiting the flow of the current leading to an increase in the dielectric loss (Revil et al., 2016). As the frequency increases, the ability of the charges to accumulate at the interfaces decreases, which will decrease the dielectric loss (Revil et al., 2016). Another observed effect is the bound water relaxation. This effect refers to the influence of water molecules held by soil particles interacting with the applied electric field (Liu et al., 2020). The strong attraction between bound water and soil particles limits the ability of this water to move and align with the electric field (Liu et al., 2020). As the frequency of the applied signal increases, the bound water molecules try to reorient but cannot follow the rapid changes, leading to higher dielectric losses (Liu et al., 2020). It is evident that the charged double layer and the ionic conductivity play major roles in the imaginary part of the soil's permittivity at low frequencies. These two effects are related to the ion concentration (Ma et al., 2023). In a situation where more than one ion species is present in the soil, they all take a role in the impedance spectrum. Additionally, the dielectric spectrum covers other soil properties such as the microgeometry of the pores and petrophysical parameters (Xu et al., 2012). Dielectric permittivity sensors and circuitry and the polarisation mechanisms will be covered later in this paper. On the other hand, the electrical conductivity of soil (EC) indicates the soil's ability to conduct electrical current. This depends on the amount of soluble salts present in the soil, known as salinity (Gong, 2022). Soil water-soluble salt, a vital indicator of mineral nutrients present in the topsoil that plants can readily utilise, plays a key role in determining whether salt ions in the soil might enhance crop growth (Gong, 2022). The value of EC is directly proportional to the concentration of salt ions in the soil within a specific range, and it is measured in milliSiemens/centimetre (mS/cm) (Gong, 2022). The source of the soluble ions is mainly fertilisers and water (Gong, 2022).

There are two types of EC in soil, bulk EC (σ_b) and pore water EC (σ_p). Bulk EC represents the total value of measured EC in the soil, including both solid particles and dissolved solution (Bañón et al., 2021). σ_p is the EC in the soil's pore space (Bañón et al., 2021). It is also known as plant-available EC, and this value is particularly significant for plants as it indicates the water and nutrients accessible for plant uptake (Bañón et al., 2021).

Soil is a matrix composed of air, pore spaces, water, and solid material (Chan, 2018). Fig. 3 illustrates three different pathways that can be taken by electrical current in soil. Pathway one represents the route of electrical current through solid (soil) and liquid (water). Conductivity is influenced by both water and soil and will rise as the water content increases (Corwin and Scudiero, 2020). Pathway two is the electrical pathway related to the electrical conductivity of liquid (water) in soil pores. EC here is directly proportional to the salts concentrations because the ions will dissolve and reside in the large pores; however, it is also affected by the quantity of water, with higher water content resulting in higher EC values (Corwin and Scudiero, 2020). Pathway three is the pathway that is attributed to the solid (soil) particles (Corwin and Scudiero, 2020). These soil particles are in continuous and direct contact with one another (Corwin and Scudiero, 2020). Due to the availability of these different pathways, the electrical conductivity of the soil is being influenced by multiple factors which will be discussed in the section entitled "Factors Influencing Soil Characteristics".

Traditionally, σ_p used to be measured by two different methods, mainly by extracting soil solution by suction or by using saturated paste conductivity measurements (Aljoumani et al., 2018). However, these techniques are costly and labour-intensive since the usage of suction cups in extracting soil solution requires a lot of time and effort, as well as, to prepare a soil-saturated paste to measure its conductivity is destructive and time-consuming (Aljoumani et al., 2018; Kamewada and Ooshima, 2024).

To avoid the complexity of the above method, the look for the development of an in-situ soil electrical characteristics measurement technique capable of measuring σ_p, started years ago. A lot of research has been done around this work, and it is found that there exists a linear relationship between the soil bulk dielectric permittivity ε_b and σ_p (Aljoumani et al., 2018). By the end of the 20th century, Max A. Hilhorst utilised the relationship between ε_b and σ_p to develop an equation that links σ_b to σ_p if ε_b is known. After the proposal of the Hilhorst equation, multiple companies started following this theory in developing soil sensors which will be discussed in the section entitled "Measurement of Soil Properties". The equation is presented as follows (Hilhorst, 2000):

$$\sigma_p = \frac{\varepsilon_p \sigma_b}{(\varepsilon_b - \varepsilon_{|\sigma_b=0})} \tag{1}$$

where ε_p is the real part of the dielectric permittivity of the soil pore water, with a value of approximately 80 (corresponding to the relative permittivity of water at 20 °C), σ_b can be directly measured using an EC sensor (will be discussed more in subsequent sections), ε_b is the real part of the dielectric permittivity of bulk soil, and $\varepsilon_{|\sigma_b=0}$ is an offset term calculated from ε_b and σ_b values obtained at two arbitrary free water content levels. ε_p can be calculated as follows (publisherCreate a flipbook, 2008):

$$\varepsilon_p = 80.3 - 0.37(T_{soil} - 20) \tag{2}$$

where T_{soil} is the measured temperature of the soil. Therefore, ε_p is a function of temperature also.

2.2. Factors influencing soil characteristics

The first influencing factor on soil characteristics is temperature. Here is an explanation of how the different electrical conductivities in soil are affected by the temperature. The bulk electrical conductivity σ_b that is measured from the soil is the sum of the conductivity of pore water σ_p and the conductivity of the diffuse double layer of soil particles surface σ_s (Ko et al., 2023). A diffuse double layer is formed by the distribution of the ions on the surface of a particle (such as clay) describing the electrical potential's variation near a charged surface, and it behaves as a capacitor (Mojid, 2011). These two types of conductivity will increase with the increase of temperature, such that an increase of 1 °C will cause a 2% increase in bulk conductivity (Ko et al., 2023). However, the factors influencing the relationship between σ_p and σ_s and temperature are completely different (Ko et al., 2023). While an increase in temperature leads to a rise in σ_s predominantly caused by improved cation mobility in the diffuse double layer, the corresponding increase in σ_p is primarily due to the decreased pore water viscosity (Ko et al., 2023). The variations in the temperature close to the surface double layer of the soil particles can lead to a large change in the electrical conductivity (Hayley et al., 2007).

The second influencing factor is soil moisture. The increase in soil moisture will affect the grain size and air space of the soil leading to an increase in the available ions consequently affecting the dielectric constant of the soil (Sriphanthaboot et al., 2021). Most soil electrical conductivity sensors work by measuring the changes in the dielectric permittivity of the soil (Sanchez et al., 2021). Any increase in water content in the soil will increase the value of the dielectric constant of the soil significantly because the difference in the relative permittivity between water and dry soil is substantial ($\varepsilon_{water} \simeq 80$ and $\varepsilon_{drysoil} \simeq 5$) (Sanchez et al., 2021; Zawilski et al., 2022).

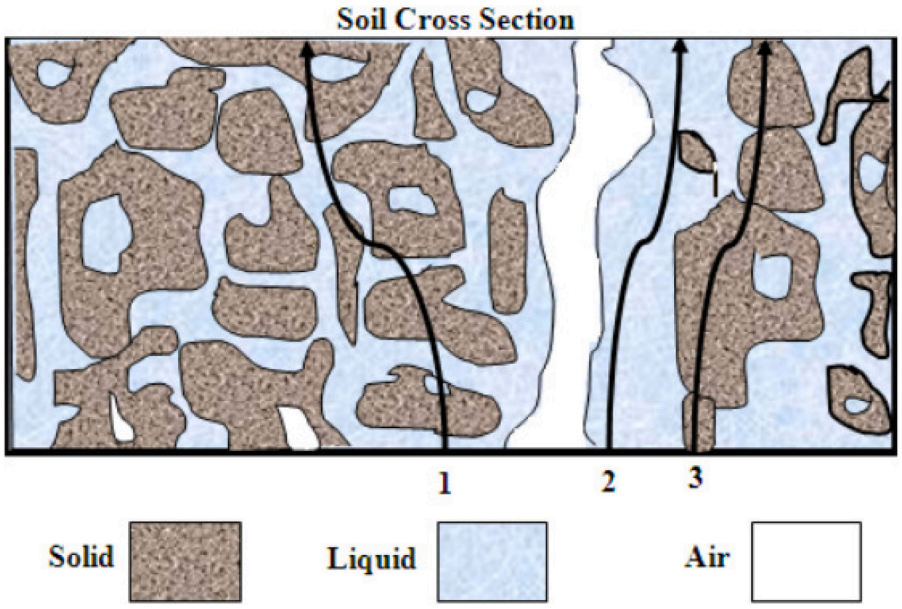

Fig. 3. Soil cross-section showing the three pathways through which charges can propagate in soil (Aljoumani et al., 2018).

The third influencing factor is the salinity levels in the soil. These levels significantly affect crop production and the overall quality of soil ecosystems in arid and semi-arid regions (Ismayilov et al., 2021). The conventional method for assessing soil salinity is by measuring the electrical conductivity of the saturated paste extract from the soil (ECe - explained in detail later) or by extracting the water from the soil sample and measuring its σ_p with a meter (Hossain et al., 2020). However, researchers and scientists follow the ECe method for the following advantages over determining σ_p; Starting with the fact that ECe is a standardised and consistent method since it involves the addition of a controlled amount of water whereas when after it is extracted by a sample its amount varies which makes measuring σ_p non standardised. Another advantage is that measuring ECe reflects the field conditions under irrigation since it gives results of the saturated soil which is the actual measure of salinity after heavy rain or after irrigation but directly measuring σ_p only provides information related to the salinity of the current soil moisture. Measuring σ_p directly from the soil extract is found to overestimate the salinity in the soil compared to the saturated paste extract method since it follows the dilution method reflecting the natural mechanisms of how salts behave in the soil after adding water. In addition, measuring ECe is a more practical method than determining σ_p because measuring σ_p directly from the soil is very challenging, especially in extreme conditions but extracting soil renders it a more practical and reliable method.

The first step of determining ECe includes the preparation of the saturated paste by air-drying the soil and then removing the large particles using a 2 mm sieve (Kargas et al., 2018a). Then, an amount of this soil is transferred to a plastic container and weighed all together. After that, the soil is mixed and stirred with deionised water until it is nearly saturated (Rhoades, 1982). The mixture is then left covered to stand for hours so the soil can imbibe the water. After several hours, more deionised water should be added to the mixture to reach a uniformly saturated soil–water paste (Rhoades, 1982). This paste should be left to stand for at least 4 h (preferably overnight), and then the criteria for saturation should be rechecked (the paste should not stiffen or lose its glisten, nor free water should be collected on the soil surface) (Rhoades, 1982). In case the saturation criteria check resulted in negative outcomes, water or soil (depending on the results) should be added to the mixture and the procedure should be followed again starting from the weigh-in step (Rhoades, 1982). Later, the paste should be transferred to a Buchner or Richards funnel with high-retention filter paper for vacuum filtration (Rhoades, 1982). The filtrate should be collected in a test tube or bottle after applying vacuum pressure (Rhoades, 1982). The filtration process should end when air begins to pass through it. After that, 1 drop of 0.1% $(NaPO_3)_6$ solution should be added for each 25 mL of extract (Rhoades, 1982). Finally, ECe can be measured by a conductivity meter (Kargas et al., 2018a). However, as mentioned earlier, this technique requires considerable time and effort due to the complex procedure. Therefore, various relationships have been established between ECe and EC of different soil–water ratios for soils from different countries (Hossain et al., 2020). Table 1 displays the relations found between ECe and EC1:5 which is EC for 1:5 soil–water ratio based on soil texture used for rapid and easy monitoring of soil salinity in an area (Gharaibeh et al., 2021). The regression equations developed in this table are used to calculate the value of ECe from EC1:5. The coefficient of determination, R^2, represents the accuracy of the developed equations. However, these equations vary with the region, type of salts, and soil texture. Therefore we cannot generalise these relations (Gharaibeh et al., 2021). The procedure followed to measure EC1:5 is simpler and less time-consuming than the one used in ECe. To develop a 1:5 soil–water ratio, we need to add 5 g of deionised water for each 1 g of air-dried sieved soil (Rhoades, 1982). Then place the mixture in a mechanical shaker for 1 h (Rhoades, 1982). After that, the mixture should be filtered using a high-retention filter paper (Rhoades, 1982). Then, the same procedure as in ECe is followed to measure EC1:5. After calculating the ECe value we can identify the salinity of the soil using the following relationships: if ECe value is less than 4 dS/m then the soil is salt-free; if ECe is between 4 and 8 dS/m, the soil is slightly saline; if ECe is between 8 and 15 dS/m, the soil is moderately saline; and if ECe is higher than 15 dS/m, the soil is strongly saline (Alonge et al., 2019).

The fourth influencing factor is soil texture (clay, silt, and sand). These soil textures can be distinguished by their particle size. However, there is a difference in how scientists classify these sizes. For instance, sedimentologists classify particles less than or equal to 4 μm as clay, while geologists typically define clay particles as 2 μm in size (Moreno-Maroto and Alonso-Azcárate, 2018). Increasing clay particles in a soil matrix will increase σ_b (Faruque et al., 2006). Loam is a soil composed of 20% clay, 40% silt, and 40% sand particles. Silt loam soil (silt particles dominating) exhibits higher electrical conductivity compared to sandy soil and sandy loam (sand particles dominating) soil due to the presence of higher quantities of clay minerals available in silt loam soil than in the two other soil mixtures (Faruque et al., 2006). Moreover,

Table 1
Reported relationships between ECe and EC of 1:5 soil–water extracts. R^2 is the coefficient of determination, and EC1:5 is the conductivity of soil–water ratio used (Gharaibeh et al., 2021; Spiteri and Sacco, 2024).

Reference	Regression equation	R^2	ECe range (dS/m)	Country/region
Richards (1954)	$ECe = 4.81 \cdot EC1:5$	0.9		USA
Herrero and Pérez-Coveta (2005)	$ECe = 7.63 \cdot EC1:5 - 0.51$	0.9	2.9–4.6	Spain/Ebro basin
Ozcan et al. (2006)	$ECe = 5.97 \cdot EC1:5 - 1.17$	0.9		Turkey
Sonmez et al. (2008)	$ECe = 7.68 \cdot EC1:5 - 0.16$	1	0.2–17.7	Turkey/Aldeniz
Chi and Wang (2010)	$ECe = 11.68 \cdot EC1:5 - 5.77$	0.9	1–227.0	China/Songnen
Khorsandi and Yazdi (2011)	$ECe = 5.40 \cdot EC1:5 - 0.61$	1	0.5–171.0	Iran/Yazd
Visconti and de Paz (2012)	$ECe = 5.7 \cdot EC1:5 - 0.2$	0.9	0.3–3.3	Spain/Southeast
He et al. (2013)	$ECe = 2.86 \cdot EC1:5 + 2.96$	0.7	0.0–17.0	USA/North Dakota
Klaustermeier et al. (2016)	$Log_{10}ECe = 1.2562 \cdot Log_{10}EC1:5 + 0.7659$	0.9	0.4–126.0	USA/North Dakota
Aboukila and Norton (2017)	$ECe = 5.04 \cdot EC1:5 + 0.37$	0.93	0.62–10.3	Egypt/Beheira
Aboukila and Abdelaty (2017)	$ECe = 7.46 \cdot EC1:5 + 0.43$	0.97	0.3–18.3	Egypt/Beheira
Leksungnoen et al. (2018)	$ECe = 5.99 \cdot EC1:5 + 0.62$	1	12.4–80.7	Thailand/Khorat & Sakhon basins
Kargas et al. (2018b)	$ECe = 6.53 \cdot EC1:5 - 0.108$	0.9	0.47–37.5	Greece/multiple locations
Jin et al. (2019)	$ECe = 8.70 \cdot EC1:5$	0.9	1–30	South Korea/multiple locations
Kargas et al. (2020)	$ECe = 6.58 \cdot EC1:5$	1	0.61–25.9	Greece/Three locations

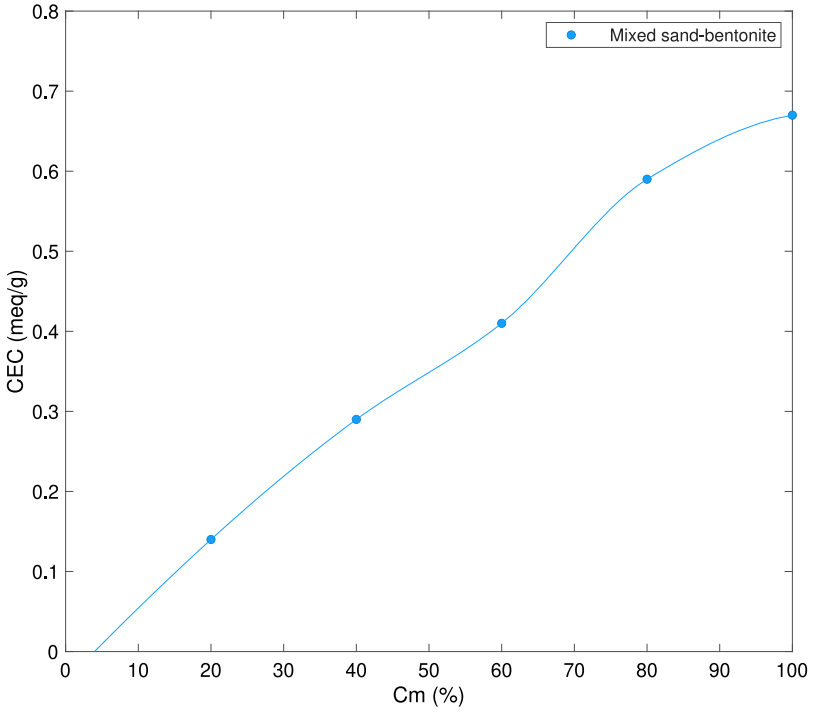

Fig. 4. Variation of CEC with clay content (meq/g stands for milliequivalent per hundred grams).
Source: Redrawn from Al-Moadhen et al. (2022).

Seo et al. have developed an equation that relates the sand content with a conversion factor (CF) used to calculate ECe from EC of soil–water extracts at a 1:5 ratio (EC1:5) (Seo et al., 2022). The following equation displays the relationship between CF and sand content (Seo et al., 2022):

$$CF = \frac{8.9105e^{0.0106sand}}{1.2984} \tag{3}$$

Electricity cannot pass through sand particles; therefore, in sandy soil, the conductivity of pore fluids is the conductivity of this soil (Al-Moadhen et al., 2022). However, electricity can pass through clay particles. So, the electrical conductivity of clay and pore fluid depends on the quantity and type of clay present, influenced by factors such as cation exchange capacity (CEC), porosity, and the conductivities of both the pore fluid and the clay (Faruque et al., 2006; Al-Moadhen et al., 2022; Choo et al., 2022).

CEC is the fifth influencing factor representing the ability of soil to hold exchangeable cations (Choo et al., 2022). The surface of clayey soil can generate electrostatic force because its surface is negatively charged (Choo et al., 2022). Therefore, clayey soil can absorb and hold cations (Choo et al., 2022).

Since σ_b will depend on the CEC of clay particles, a relationship between CEC and clay content should be investigated. The following figure illustrates the relationship between CEC and clay content (C_m). In Fig. 4, the CEC of mixed sand-bentonite was measured by varying the content percentage. The relation between CEC and clay content is directly proportional. Therefore, an increase in clay content will result in a corresponding increase in CEC, leading to an increase in σ_b. Moreover, the inorganic content (minerals), plays a role similar to ion concentrations in altering the value of the electrical conductivity in the soil. Soil having clay minerals with high CEC, such as smectite, results in higher σ_b than the ones with lower CEC, such as kaolinite (USDA-NRCS, 2024).

As previously mentioned, the bulk electrical conductivity, σ_b, is the sum of σ_s and σ_p. Both σ_s and σ_p depend on porosity n, which reflects the volume fractions of pore space. This is presented in the following equation (Choo et al., 2022):

$$\sigma_b = \sigma_p + \sigma_s = \sigma_p n^m + \lambda(1-n)^p \tag{4}$$

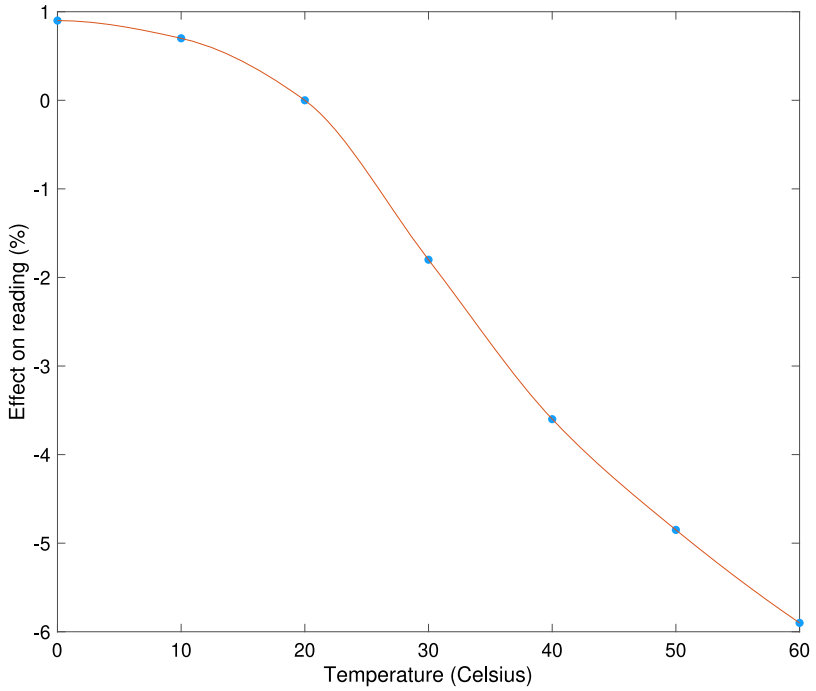

Fig. 5. Effect of soil matrix temperature on ϵ, expressed in % full scale (ϵ = 80), with 20°C taken as reference. *Source:* Redrawn from Balendonck et al. (2021).

where the matrix conductivity is represented by λ; the volume fraction of solid particles is $1-n$; m represents the shape factor for pore water conductivity; and p is the shape factor for surface conductivity. The increase in porosity n will increase the connectivity of pore space which will increase σ_b.

The sixth influencing factor is the organic matter content, such as crop residue, livestock manure, green manure, compost, humus, and their combination, which is regarded as a substitute for chemical fertilisers. It is considered a sustainable horticultural practice because it can enhance microbial biomass and associated activities, soil fertility, and crop productivity (Shu et al., 2022). The relationship between organic matter content and electrical properties is quite complex. However, based on a study done by Iranmanesh and Sadeghi in 2019, organic matter and electrical conductivity are negatively correlated (Iranmanesh and Sadeghi, 2019). Therefore, an increase in soil's organic matter content will lead to a decrease in the electrical conductivity because the soil moisture will decrease due to the metabolic processes undertaken by the microbes and living organisms in the soil (Trigona, 2020).

2.3. Limitations of soil theory

From the theory relating to soil electrical conductivity, it is apparent that pore water electrical conductivity is of primary interest since the conductivity of pore water contains a lot of information related to the health of the plants. In addition, σ_p directly reflects the quantities of the dissolved salts and water that are ready to be consumed by the plants. This electrical characteristic depends on various factors, but the most significant ones are ε_p and $\varepsilon_{|\sigma_b=0}$. Following Hilhorst's findings, the values of $\varepsilon_{|\sigma_b=0}$ can range from 3.1 to 7.6, and it was suggested using $\varepsilon_{|\sigma_b=0}=4.1$ as an average value to facilitate calibration (Hilhorst, 2000). However, under saline conditions, the accuracy of a sensor to predict σ_p is very poor using this standard value (Zemni et al., 2022). Hamed et al. found that by using the default value proposed by Hilhorst (4.1), the estimated value of σ_p is 20% of the true value when $\sigma_p > 1dS/m$ (Hamed et al., 2003).

Many factors can contribute to this significant inaccuracy, for instance, the offset value ($\varepsilon_{|\sigma_b=0}$) should not be fixed since each type of soil mixture has a different $\varepsilon_{|\sigma_b=0}$ value. This was illustrated in multiple studies done by different researchers as Magnus Persson used different values in his study in 2002 for different soil types ranging between 3.67 and 6.38 and later Decagon Devices, Inc., Pullman, WA used an offset of 6 (Aljoumani et al., 2015). Then in 2009 Arquedas-Rodriguez used the sensor developed by Decagon Devices and found that the relation is nonlinear for the chosen offset (Aljoumani et al., 2015). Moreover, in 2009, Bouksila et al. used the WET sensor (Delta-T Devices Ltd, Cambridge, UK) which is a frequency domain dielectric sensor designed for use with offset proposed by Hilhorst ($\varepsilon_{|\sigma_b=0}=4.1$), and found difficulty in predicting ε_p in saline gypsiferous soil (Aljoumani et al., 2015). Furthermore, Al Joumani et al. have applied a new stochastic model to find the relation between ε_p and $\varepsilon_{|\sigma_b=0}$ and they have discovered that in the same soil profile, the offset was varying with depth. This can be attributed to the change in the soil's temperature (Aljoumani et al., 2015). So, the offset value is not only changing between soil types but it is changing within the same medium also depending on the soil since water can quickly flow downwards. Another key element could be ε_p which is influenced by soil temperature as shown in Fig. 5. Furthermore, both σ_p and σ_s (the ionic conductivities) are sensitive to temperature variations. Additionally, the ionic conductivities are influenced by the soil texture, porosity, CEC, organic matter content, and inorganic matter content. All the previously mentioned factors are assigned specific values in Hilhorst's equation (Eq. (1)). σ_b is influenced by the salinity, and when the moisture of the soil mixture changes, σ_p calculated using Eq. (1) does not reflect the actual salinity (Bañón et al., 2021). So, the Hilhorst model used to estimate ε_p has limitations when applied in saline soils, because this model may lead to inaccurate predictions of ε_p due to the altered behaviour of ions in the soil solution. The developed model does not account for this change adequately.

The Hilhorst equation requires that pore water conductivity dominates the bulk conductivity measurement, a condition that is not met in many real-world scenarios, for instance the availability of conductive soil particles such as clay will exhibit high electrical conductivity even in the absence of water (Goodchild, 2023). In addition, the Hilhorst model does not take into consideration the surface conductivity of solid particles, which could add to the error in estimating σ_p (Zemni et al., 2022).

The interference from the environment such as external factors (temperature, salinity, vegetation, microorganism, and fungal content) impacts the electrical properties of the soil by introducing noise and affecting the measurement accuracy. In addition, soil type influences the determination of the soil's electrical characteristics because different soil types exhibit distinct electrical behaviours. For instance, sand-rich soils behave in a different way from clayey soils, affecting dielectric measurements. So, the understanding of each specific soil type is essential for accurate calibrations and interpretations.

The theory behind the soils' dielectric properties is incomplete and complex. Excessive assumptions in a single model for measuring electrical conductivity can lead to substantial errors. Therefore, efforts should be directed towards minimising assumptions to achieve higher levels of accuracy. In addition, soil should not be considered a uniform medium because of differences in moisture, structure, and composition. As such, the dielectric measurements will be affected by these inhomogeneities.

3. Measurement of soil electrical properties

The subsequent section will examine the measurement techniques currently available in the market. Additionally, the challenges and limitations associated with these techniques will be analysed and compared with the traditional method. Moreover, this section will also address the challenges and theoretical aspects of measuring electrical properties at the system level.

3.1. Measurement techniques

This section is divided into many subsections to cover the most commonly used approaches to measure soil's electrical characteristics. The measurement techniques that are mentioned in this part are as follows: traditional measurement techniques, capacitive sensors, time domain reflectometry, frequency domain reflectometry, amplitude domain reflectometry, and broadband dielectric spectroscopy. Each method will be described and analysed to provide the limitations and challenges of it.

3.1.1. Traditional measurement techniques

Gravimetric and volumetric methods are the direct techniques used traditionally to estimate soil moisture. The gravimetric technique requires time and labour since the soil sample should be removed from the ground, weighted, heated at 100 °C in an oven for 24 h to get dry, and weighted again, so the weight of the soil with and without the water can be obtained to calculate its water content (Tomar and Patidar, 2019). Alternatively, the same procedure can be applied at 60 °C for 48 h (Robertson and VanderWulp, 2024). The following formula is used to calculate the moisture M in the soil sample using the gravimetric technique (Tomar and Patidar, 2019).

$$M(\%) = \frac{x - y}{y} \times 100 \tag{5}$$

where x is the weight of wet soil, and y is the weight of dry soil. Whereas, the volumetric soil moisture content is represented by the ratio of the volume of moisture available in the soil sample to the total volume of the same sample, by following the same procedure as in the gravimetric technique (Susha Lekshmi et al., 2014). Alternatively, we can get the volumetric water content indirectly by using a sensor capable of measuring the dielectric constant, electric resistance, or electrical conductivity (Tomar and Patidar, 2019). Midday Stems Water Potential (SWP) is the most widely accepted method to determine the status of water for a crop (González-Teruel et al., 2022). SWP is used to assess the status of water relevant to the plant indicating the pressure or the tension exerted by the plant to pull water up from the roots (Moriana et al., 2012). However, this technique is costly and soil-destructive in terms of associated labour, time, the machinery used (pressure chamber), and the procedure of taking the plants from the soil (González-Teruel et al., 2022). Therefore, researchers are trying to find an indirect way to measure SWP by creating a relationship with other agro-climatic variables such as air temperature, solar radiation, and vapour pressure (González-Teruel et al., 2022).

Nitrate, like other types of fertilisers used in agriculture, play a critical role in boosting crop yield and ensuring food security globally. It has been measured using soil sampling and subsequent laboratory analysis. This traditional approach is expensive and requires significant labour resources as it requires a specialist capable of developing a comprehensive soil sampling protocol and thorough laboratory sample diagnosis (Bellosta-Diest et al., 2022). Recently, ion-selective electrodes, a type of electrochemical electrode, were being used to measure the nitrate concentrations in soil (Bristow et al., 2022). However, this method has several disadvantages, mainly the electrodes are weak and the system requires continuous calibration. For instance, the measurements taken using this type of sensors remained stable for only the first six weeks post-deployment, after which the values started to drift (Bristow et al., 2022).

In addition to the measurement techniques discussed above, there are numerous dielectric measurement techniques available for obtaining σ_b and ε_b values, which are critical parameters for applying the Hilhorst equation (Eq. (1)). Capacitive sensors, impedimetric sensors, time domain reflectometry, frequency domain reflectometry, amplitude domain reflectometry, and broadband dielectric spectroscopy techniques will be discussed in the following subsections.

3.1.2. Capacitive sensors

The galvanic cell method is widely used in soil moisture sensors (Pieris and Chathuranga, 2020). This method relies on the generation of voltage resulting from the redox reactions occurring between two dissimilar metals inserted into the soil. However, the electrodes eventually corrode in a prolonged operation (Pieris and Chathuranga, 2020).

To overcome this issue, capacitive sensors (Fig. 6) are utilised to measure the dielectric properties of the soil.

Fig. 6 illustrates the circuitry and the injected electrodes of a capacitive sensor. The principle behind capacitive sensors is illustrated by the following equation; assuming a model of a parallel plate capacitor:

$$C = \frac{A\varepsilon}{d} \tag{6}$$

where C is the capacitance, A is the area of the surface of each plate, d is the distance separating the two plates, and ε is the dielectric permittivity of the material between the plates (soil in our case). Whenever the soil moisture changes, the dielectric constant of the soil will change, resulting in a change in the capacitance.

There are different methods to measure capacitance. For instance, Pieris and Chathuranga (2020) have used a stable multivibrator circuit to generate a square-wave output, from which they could derive the capacitance. This circuit generates a square wave signal influenced by the sensor's capacitance, which is impacted by the soil's dielectric constant. The sensor's capacitance, C, alters the duration during which the signal is high in the square wave, t_H, denoted according to the relation below (Pieris and Chathuranga, 2020):

$$C = \frac{t_H}{0.693(R_1 + R_2)} \tag{7}$$

t_H was measured by a microcontroller, R_1 and R_2 are the resistors used in the circuit (1 kΩ both).

Goswami et al. (2019) have developed a circuit capable of reading the soil moisture levels using a capacitive sensor and a capacitance-to-voltage converter (Fig. 7).

Fig. 7 shows the soil moisture sensor's block diagram, representing the capacitive sensor's signal conditioning circuit (Goswami et al., 2019). An AC excitation signal with low frequency is used to excite the bridge. Then a peak detector is used to capture the different amplitude and phase generated from the probes.

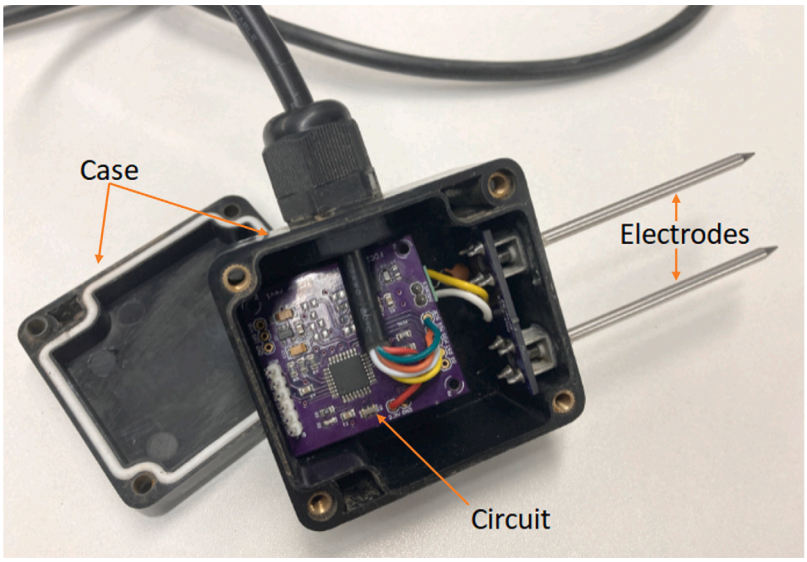

Fig. 6. Circuit and probes of the capacitive sensor.
Source: Redrawn from Sanchez et al. (2021).

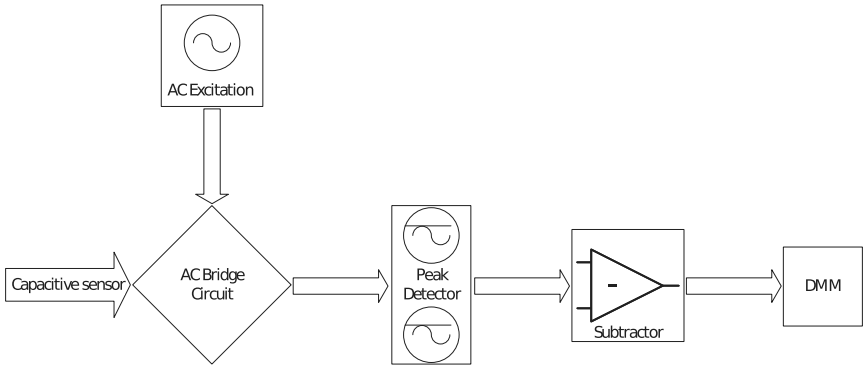

Fig. 7. Block diagram of soil moisture sensor.
Source: Redrawn from Goswami et al. (2019).

The output voltage of the peak detectors is then subtracted using a subtractor, and a digital multimeter is used to measure the difference. Subsequently, the system output voltage is calculated using the following equation (Goswami et al., 2019):

$$V_{out} = \frac{a(bC_s - 1)}{a^2C_s + abC_s + b + a} V_{in(p)} \tag{8}$$

where $a = 2\pi f R$, $b = 1/C$, C represents the capacitance of the used capacitor in the circuit, $V_{in(p)}$ is the peak voltage of the bridge excitation signal, and C_s is the capacitance of the soil moisture sensor.

Other researchers have also developed capacitive soil sensors to measure nitrate values using different shapes of sensors. For example, Sanket et al. (2018) have developed a low-cost nitrate detection soil sensor that is star-shaped (Sanket et al., 2018). The concept and circuitry of their system are similar to those displayed in the previous figures; however, they have modified the configuration to enhance sensitivity.

3.1.3. Time domain reflectometry

Time-domain reflectometry (TDR) is an increasingly used technique for measuring soil moisture (Abdullah et al., 2018). TDR operates based on the principles of radar systems, measuring and recording the propagation of electromagnetic waves. The underlying idea of this technique involves transmitting an impulse and then observing the time it takes for the response. So, the first step in TDR measurement is to send a signal through the probes to the soil (Walczak and Lipiński, 2021). Then, since the medium (soil in our case) is not a full conductor and its dielectric constant varies with the different water concentrations, the speed of the reflected signal will be different from the generated one (Walczak and Lipiński, 2021). In dry soil, minimal reflections will occur and the signal will reflect at the same speed as generated (Walczak and Lipiński, 2021). Conversely, in wet soil, the signal will encounter more water molecules which will reflect more of the signal and make it slower (Walczak and Lipiński, 2021). The time taken for the reflected signal to travel back to the TDR is measured (Walczak and Lipiński, 2021). Knowing the speed of the pulse in the dry soil, the measured time of the reflected signal is used to calculate the dielectric constant of the soil following some calibration equations which will be discussed later in this section (Walczak and Lipiński, 2021).

A typical TDR measurement setup comprises a TDR device and a transmission line system. The TDR device typically includes a pulse generator, a sampler, and an oscilloscope (Lin et al., 2010). The transmission line system consists of a probe connected to the TDR device via a coaxial cable (Lin et al., 2010). Fig. 8 displays a typical setup for a TDR measurement. The step generator sends an electromagnetic pulse along the coaxial cable. Subsequently, the sampler records the reflected signal from the probe, which occurs due to an impedance mismatch between the probe and the soil (Lin et al., 2010).

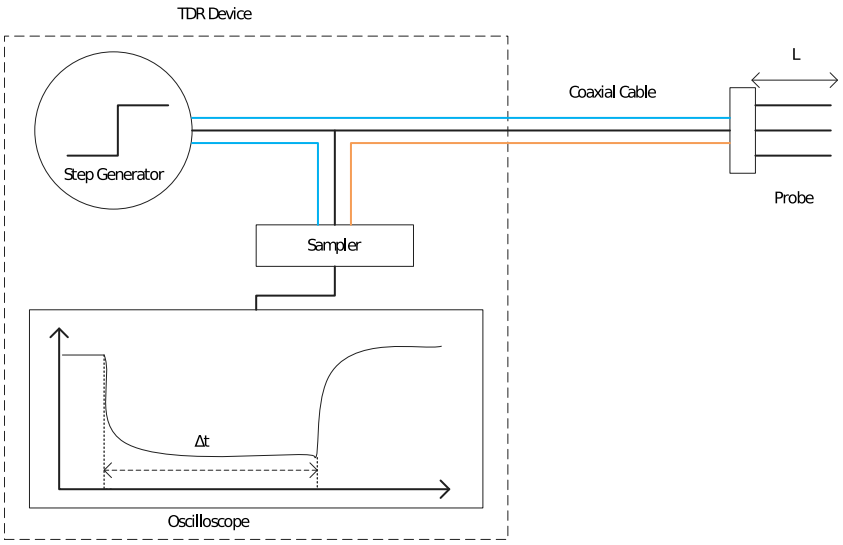

Fig. 8. Time Domain Reflectometry (TDR) measurement setup.
Source: Redrawn from Lin et al. (2010).

In the model mentioned in Fig. 8, the dielectric constant of the mixture (air, soil, and water) ε can be calculated as follows:

$$\varepsilon = (\frac{ct}{2L})^2 \tag{9}$$

where t is the transit time for the signal to propagate and reflect along the probe's length L, and c is the speed of light in a vacuum (Regalado et al., 2003). In 1980, Georges C. Topp generated an empirical model to estimate the volumetric water content θ_v of soil where he relates the measured dielectric permittivity of the soil at a specific frequency to θ_v (Topp, 1980). Then θ_v can be calculated using the empirical model given by Topp (Abdullah et al., 2018) using the following relation:

$$\theta_v = (-530 + 292\varepsilon - 5.5\varepsilon^2 + 0.043\varepsilon^3) \times 10^{-4} \tag{10}$$

3.1.4. Frequency domain reflectometry

The elements that form the frequency domain reflectometry (FDR) system are similar to the ones for TDR.

The FDR system typically consists of an FDR probe, a coaxial cable, and a magnetic wave generator (Minet et al., 2010). The wave generator produces a signal, which is then transmitted to the probes via the coaxial cable. The FDR probes serve as a coaxial medium in which an AC signal oscillates between the external and central rods, with the soil serving as the insulating material of the coaxial line (Minet et al., 2010). The internal electromagnetic properties (permittivity, conductivity, and susceptibility) and dimensions, characterise each sequential element of the FDR system to determine the complex impedance (Minet et al., 2010). Any change in one of these properties will result in a change between the transmitted and the reflected wave signal (Minet et al., 2010). When a wave signal propagates through an inhomogeneous medium, the signal will be scattered and the reflected signal will change from the original signal (Geyer and Karastergiou, 2016). A vector network analyser (VNA) is a device used with the FDR system to measure the frequency-dependent scatter function representing the ratio between the reflected signal and the transmitted signal (Minet et al., 2010). Fig. 9 displays a typical FDR system.

The complex dielectric constant (ε^*) can be calculated as follows:

$$\varepsilon^* = \varepsilon_r - j\varepsilon_i \tag{11}$$

where the real part of the equation ε_r represents the polarisability or the capacitive characteristics of the soil, and the imaginary part ε_i represents the losses contributed to conductivity and polarisation (Xu et al., 2012). ε_i is the result of molecular relaxation and electrical conductivity, and it is represented by the following equation:

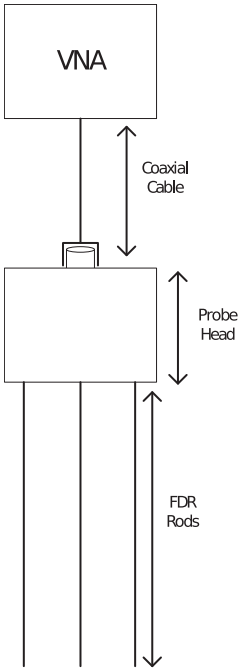

Fig. 9. Typical FDR system with VNA.
Source: Redrawn from Minet et al. (2010).

$$\varepsilon_i = \varepsilon_{ird} + \frac{\sigma_{dc}}{2\pi f \varepsilon_0} \tag{12}$$

where ε_{ird} represents the loss factor caused by the dielectric relaxation losses, σ_{dc} in (S/m) represents the soil's electrical conductivity when DC signal is applied, f is the measurement frequency in Hz, and ε_0 is the dielectric constant of vacuum (8.854×10^{-12} F/m) (Xu et al., 2012). From the above equations, it can be concluded that ε^* depends on the soil's electrical properties, including its DC electrical conductivity and frequency of the applied signal. Debye and Cole-Cole models describe the relationship between these factors and it is summarised in the

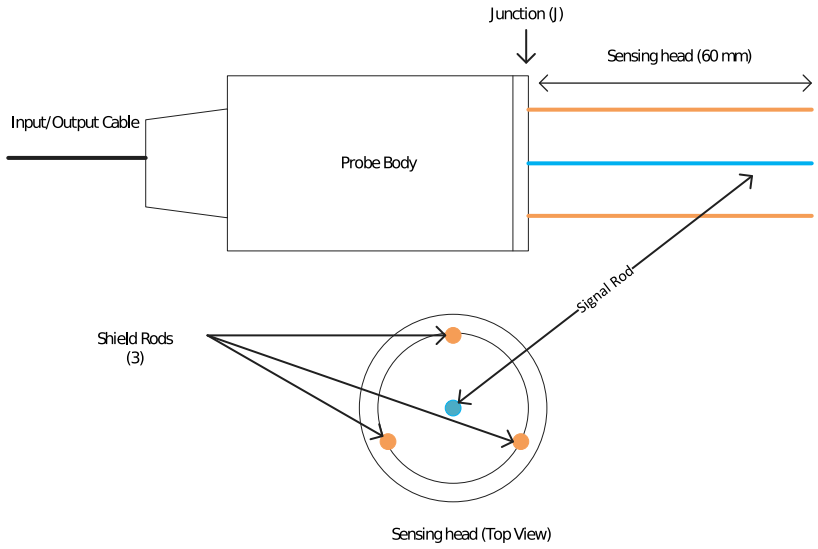

Fig. 10. Amplitude Domain Reflectometry (ADR) measurement setup.
Source: Redrawn from Wijaya et al. (2003).

following equation (Xu et al., 2012):

$$\varepsilon^*(f) = \varepsilon_\infty + \frac{\varepsilon_s - \varepsilon_\infty}{1 + (\frac{if}{f_r})^{1-\beta}} \tag{13}$$

where ε_∞ and ε_s represent the values of ε_r at high and low frequencies, respectively, f_r is the relaxation frequency, and β represents the exponent describing the spread of the relaxation peak (the permittivity of a soil sample changes with the frequency change of an applied AC field where in some cases the permittivity might show a peak at a specific frequency range representing the delayed or lagged process of the soil's response at that particular frequency) (Xu et al., 2012).

3.1.5. Amplitude domain reflectometry

Amplitude domain reflectometry (ADR) implements a similar approach as in TDR and FDR but here the amplitude of the reflected signal is captured and analysed. ADR is usually composed of three major components: a sensing head, a probe body, and an input and output cable (Fig. 10). The cable provides a power supply to the system and a connection for the analogue signal output. An oscillator, measuring circuitry, and a specially designed internal transmission line are contained in the probe body within a waterproof housing. The sensing head includes an array of four electrodes (the outer three electrodes are connected to the ground and the central electrode is used for the signal) (Wijaya et al., 2003). Fig. 10 represents a typical ADR setup.

The working principle behind the ADR is similar to the one in TDR but here the amplitude of the reflected signal is captured. First of all, an ADR probe is inserted in the soil to act as a transmission line with a specific impedance. Then, a high-frequency sinusoidal signal (around 100 MHz) is sent into the soil down the probe. The electrodes' impedance depends on the soil's dielectric constant (including its water content) surrounding it. When the impedance of the surrounding environment differs from that of the transmission line creating an impedance mismatch at the soil-probe interface, a proportion of the transmitted signal will be reflected from the junction (J) which lies between the transmission line and the sensing array. The reflected signal will interfere with the generated signal which will lead to a variation in the voltage amplitude along the length of the line. After that, the ADR system will measure the attenuated and reflected pulse. Then, the measured amplitude and travel time are used to find the relative impedance of the probe and hence the dielectric constant of the soil will be known. The soil's volumetric water content measured by ADR (θ_{ADR}) can be determined following the below equation (15) (Wijaya et al., 2003):

$$\theta_{ADR} = 0.00111 + 1.531\upsilon - 2.342\upsilon^2 + 1.448\upsilon^3 \tag{14}$$

where υ is the output voltage measured from the ADR probe. However, θ_{ADR} depends significantly on the type of the soil (Wijaya et al., 2003). Moreover, the relationship between the output voltage and the dielectric constant is illustrated in the following equation (16) (Wijaya et al., 2003):

$$\sqrt{\varepsilon} = 1.07 + 6.40\upsilon - 6.40\upsilon^2 + 4.70\upsilon^3 \tag{15}$$

where $\sqrt{\varepsilon}$ is the square root of the dielectric constant of the soil matrix.

3.1.6. Broadband dielectric spectroscopy

Broadband dielectric spectroscopy (BDS) or electrical impedance spectroscopy (EIS) is another technique used to analyse the properties of conductors, semiconductors, and insulating materials. It employs a similar concept to TDR and FDR for obtaining the complex dielectric constant. However, instead of a single frequency, a range of frequencies is used. It has been demonstrated that employing various frequencies to capture the magnitude and phase of the electromagnetic signal can facilitate the determination of multiparameters in porous media (González-Teruel J.D. Jones et al., 2022a).

The potential applicability of this technique in soil monitoring is justified by the fact that soil is composed of three phases, liquid, solid, and gaseous. This results in a relative permittivity, or a dielectric constant, ranging from 2 to 14, depending on the soil, knowing that water is a polar liquid with a high dielectric constant (≈80) at room temperature. The liquid phase is represented by the ion solution with nutrients available in the soil, necessary for the fertility of the medium and it has a high static dielectric constant, which is inversely influenced by the concentrations of the ion (Ma et al., 2023). When the ion concentration increases, the ions make the water molecules oriented around them, which will reduce the dielectric constant to 40 by a local high-field effect (Ma et al., 2023).

This technique is based on the dielectric properties of the tested material, focusing on the distribution of internal and external electric charges and their interaction with an induced electric field. EIS measurements provide electrical properties in two different ways: either through an equivalent electrical circuit consisting of inductive, resistive, and capacitive elements or by providing an effective complex dielectric constant (Kadan-Jamal et al., 2020). In an AC electric field,

the soil solution mixture will absorb and store energy. The real part of the permittivity relates to energy storage effects, whereas the imaginary component of the permittivity relates to energy absorption.

3.2. Challenges and limitations of measurement techniques

All the previously mentioned methods for measuring the electrical properties of soil come with their own set of limitations and challenges. For instance, capacitive sensors demonstrate limited accuracy which can vary depending on the composition of the soil mixture and temperature variations (Nagahage et al., 2019; Morais et al., 2019). Capacitive sensors require good contact with the soil to avoid air gaps, as some tests have shown that gap-graded soil can result in inaccurate soil moisture readings (Teixeira Ricardo Correia dos Santos et al., 2021). It is not recommended to use capacitive sensors technology for compacted soil moisture measurements in field conditions as these sensors are effective only for fine-grained soils and require proper calibration procedures (Teixeira Ricardo Correia dos Santos et al., 2021). Soil texture plays a key role in determining the soil water content using dielectric techniques (González-Teruel et al., 2019). The type of soil influences the sensitivity of this type of sensor because of the non-homogeneity characteristic of the soil (Dey et al., 2022). In addition, pores play a critical role in determining the electrical conductivity of the soil because the capacitance captured by the sensors is lower when the air has a higher void in contact with the sensor electrodes (Teixeira Ricardo Correia dos Santos et al., 2021). Also, capacitive sensors are strongly affected by the water salinity impacting the accuracy (Placidi et al., 2023). Therefore, each soil type needs a specific calibration procedure. In addition, it is necessary to use and install multiple capacitive soil sensors to correctly measure soil moisture within an agriculture field to solve the problem induced by the heterogeneous nature of the soil since each calibration curve only works for a specific soil type and characteristics (Souza et al., 2020).

Moving to the technological challenges and limitations of capacitive sensors, we can find that the feeding terminals of the plates should be addressed properly in the layout of the sensor because it is found that this can directly impact the self-resonance frequency of the sensor due to parasitic inductance (Da Costa Junior et al., 2021). In addition, multiple studies resulted in very low accuracies, for instance, the sensor developed by Pieris and Chathuranga in 2020 has a 34% error according to their calibration and evaluation (Pieris and Chathuranga, 2020). Another technical limitation of the capacitive sensor is the shape of the sensor since it is proposed that the change in the capacitance of the soil sensor relies only on the change in the dielectric constant in the soil. This was not the case in the study done by Biswas et al. in 2022, where the width of the electrodes altered the results (Biswas et al., 2022). At high frequencies (>10 kHz), the dielectric constant of the soil is small and becomes independent of the soil moisture because the capacitance of the soil is less at higher frequencies due to the polarisation of the water molecule on the surface of the sensor unable to catch up with high-frequency rate (Surya et al., 2019). Capacitive sensors are only capable of measuring the soil water content and are unable to provide further details related to the different soil properties (Shigemasu et al., 2022). In addition, capacitive sensors have limitations in measuring in-depth soil characteristics because this type of sensor is capable of measuring soil moisture near the surface of the inserted electrodes in the soil.

On the other hand, using time-domain reflectometry-based techniques incurs high costs (Dey et al., 2022). TDR systems consist of many instruments and subsystems as explained previously, making the device large and costly (Shigemasu et al., 2022). Implementing TDR sensors over an entire agricultural field is extremely costly, which can limit the widespread adoption of such a measurement technique (Biswas et al., 2022). Moreover, the penetration of TDR and FDR sensor probes into the soil can easily damage their needle-like electrodes (Xu et al., 2022). Also, dielectric measurement methods like TDR encounter challenges related to accuracy limitations, restricted sensing volume, and difficulties in achieving depth resolution (Zhu et al., 2021). Furthermore, TDR sensors may not perform well in high saline environments, as the signal reflection is restricted due to the high electrical conductivity in such conditions (Chan, 2019). Environmental conditions sensitivity and salinity limit the accurate performance of TDR technology (Tomar and Patidar, 2019). Soil moisture measurements resulting from TDR can also be affected by local ion concentration in water and the alterations done by the presence of the actual sensor in the soil (Shen et al., 2019). In addition, in a heterogeneous medium, the increased number of stones in the soil can cause trouble with the installation of the TDR probe and it can result in false measurements (Loewer et al., 2014).

FDR technologies share common drawbacks with TDR, including sensitivity to soil salinity and the need for soil-specific calibration due to variations in soil texture and bulk density (Yu et al., 2021). FDR sensors require soil-specific calibration before their installation in the soil (John et al., 2021). However, this type of calibration requires a tedious job-consuming lot of labour work, and it does not reflect the actual field conditions (John et al., 2021). FDR sensors are relatively sensitive to soil temperature, have a small sampling volume, and do not work well in some soils (Bangi et al., 2021). In addition, multiple factors have been reported affecting the FDR sensor, for instance, water quality (dissolved oxygen, temperature, organic matter content, and electrical conductivity) has been reported to alter the readings of the sensor (Zemni et al., 2022).

Furthermore, ADR techniques have the same drawbacks as FDR and TDR in terms of sensitivity towards air gaps, stones, or water travelling through channels (Mukhlisin et al., 2021). In addition, the studies done by Wijaya et al. stated that θ_{ADR} depends significantly on the type of soil and they only used two different types. So, a soil-specific calibration equation should be established in order to use this system. Moreover, this study revealed higher accuracy measurement results using a specific relationship between the water content and the measured voltage compared to using the generalised equations developed by Topp et al. leading to more complexity and incurring high costs for implementation (time and labour work).

These in situ soil moisture sensors are only capable of measuring the moisture at one single point and are unable to get complete measurements along the soil depth (Xu et al., 2018). In addition, the bulky shape of these sensors often disturbs the original texture of the soil causing errors in the measurements (Xu et al., 2018).

Like all measurement techniques, BDS has its drawbacks. Firstly, for accurate measurements, the electrodes must maintain good electrical contact with the soil (Popov et al., 2022). Additionally, the salinity of the medium can increase the EC, therefore affecting and potentially dominating the BDS spectra (Popov et al., 2022). Furthermore, soil heterogeneities can distort dielectric spectra by causing a polarisation effect at the interface, thus complicating data interpretation (Popov et al., 2022). In addition, the availability of more than one ionic species will contribute and change the impedance spectrum imposing a challenging problem in chemical sensing (Ma et al., 2023).

As we can see from the above analysis, all these different measuring techniques are used to measure the dielectric characteristics of the soil to provide useful information related to the soil's electrical characteristics. Additionally, they share common drawbacks, such as sensitivity to salinity, the need for proper soil contact, and limited sensing volume. Moreover, these different soil electrical characteristics measurement techniques require some sort of calibration to provide reasonable results. On the other hand, the traditional method to measure soil moisture remains the only accurate method available in the market. Although the traditional method requires a lot of effort and time, researchers and engineers are still relying on this method to calibrate their developed devices. Hence, exploring the causes of these limitations is crucial to enhance sensor performance.

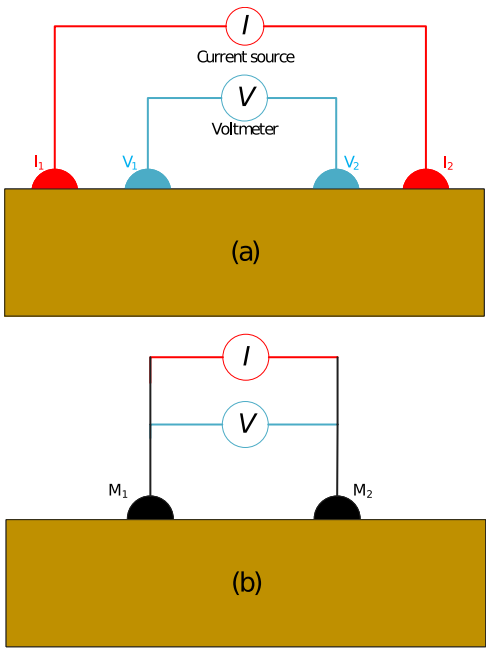

Fig. 11. Electrical impedance spectroscopy measurements electrodes configuration. (a) Four-electrode technique. (b) Two-electrode technique. "I" denotes the injection electrode, "V" is the measurement electrode, and "M" is a mixed electrode for injection and measurement.
Source: Redrawn from Bera (2014).

3.3. Theory and challenges of the electrical properties measuring techniques at system level

This review article has thus far presented the limitations of the most commonly applied soil electrical characteristics measuring techniques related to the impedance and the dielectric properties of the soil. However, all these technologies have more problems at the system level. The following section discusses the theory of the systems to measure the electrical properties of a medium and their sources of errors. The three main stages of impedance measuring techniques (injection, load, and output) will be critically analysed in the following subsections.

To calculate the impedance of the soil we have to inject a current/voltage into the soil via electrodes and measure the resulting output voltage. Then we will be able to calculate the impedance of the medium by applying Ohm's law. Two different electrode configurations are being widely used in impedance measuring techniques. Fig. 11 represents the electrode configurations being used (Bera, 2014). The medium's impedance measuring process is done by either the four-electrode or the two-electrode method. In both methods, the electrodes that inject the current are labelled as driving electrodes and the electrodes used to read the potential difference are called sensing electrodes. From their names, to measure the soil's impedance, the two-electrode method uses only two electrodes so the signal injection and measurement are done via the same electrodes (Bera, 2014). The four-electrode configuration uses two separate pairs of electrodes; two to inject and two to measure, hence this method is represented as an impedance measurement technique with a linear array of four electrodes (Bera, 2014). The four-electrode method is developed as a solution for the problems faced with the two-electrode method which will not be covered since it is out of the scope of this review. In the context of system-level electrical property measurement techniques, as previously mentioned, there are three distinct stages, each presenting unique challenges. These different stages will be covered in the following paragraphs.

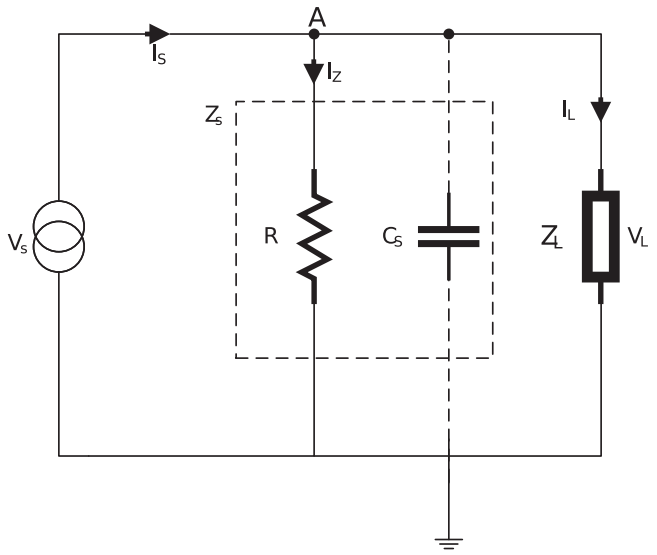

Fig. 12. Ideal model of a current injection source with the stray capacitance.
Source: Redrawn from Bertemes-Filho (2018).

3.3.1. Injection stage measuring technique

The nature of the driving signal is current. There exist multiple configurations for the injection part but they all follow the current injection method. The ideal model of a current injection source is represented in Fig. 12 (Bertemes-Filho, 2018).

In Fig. 12, V_s is the controlled input voltage, I_s is the output current of the current source controlled by V_s, Z_s represents the output impedance of the current source, C_s is the stray source capacitance, and Z_L is the load impedance which will be discussed in details later. Generally, a voltage-controlled current source (VCCS) circuit is used to convert a sine wave voltage V_s into an AC current I_L which is not affected by the load voltage V_L. The voltage at node A is equal to the load voltage and I_s is the summation of I_z and I_L ideally. However, in practice, at high frequencies, the stray capacitance C_s decreases the magnitude of Z_s which will decrease I_L (Bertemes-Filho, 2018). Therefore, it is very challenging to develop a VCCS capable of maintaining high output impedance at high frequencies.

Another current injection configuration is the improved Howland current generator topography (Fig. 13).

In Fig. 13, resistors are used to achieve an infinite output impedance (ideally) if the resistors are equal. Furthermore, a lot of researchers tried to enhance this topology to reduce the errors faced but with no positive results. The errors associated with the injection part are numerous, mainly, the output impedance will be limited due to the mismatching between the input resistors, stray capacitance, and the frequency (Bertemes-Filho, 2018). In addition, the output voltage across R_L is limited by the closed-loop gain and the supply voltages. High values of load will put the output of the operational amplifier in saturation mode, which will affect the performance of the VCCS. Moreover, despite the efforts put in to overcome these challenges, it is very hard to prevent the circuit from oscillating at high frequencies (≥1 MHz) since it is very difficult to maintain the output impedance high over a whole frequency range. Other problems were raised when multifrequency systems were required (Bertemes-Filho, 2018). A lot of detailed adjustments must be made to the feedback network to raise the output impedance and retain its stability. Some researchers introduced a buffer (voltage follower) in the feedback loop (Bertemes-Filho, 2018). However, over a wide range of frequencies, current generators do not have a constant output current nor high impedance at the output. Another source of error found is related to the common-mode voltage appearing as an unwanted potential caused by the impedance

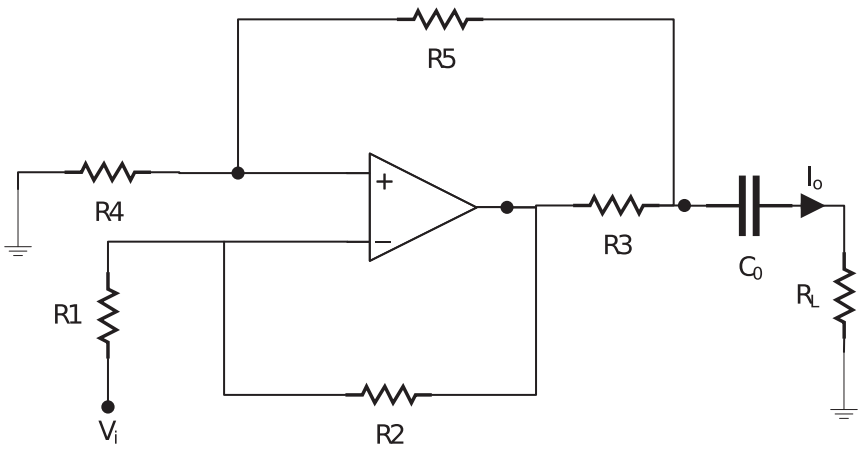

Fig. 13. Improved Howland injection module.
Source: Redrawn from Bertemes-Filho (2018).

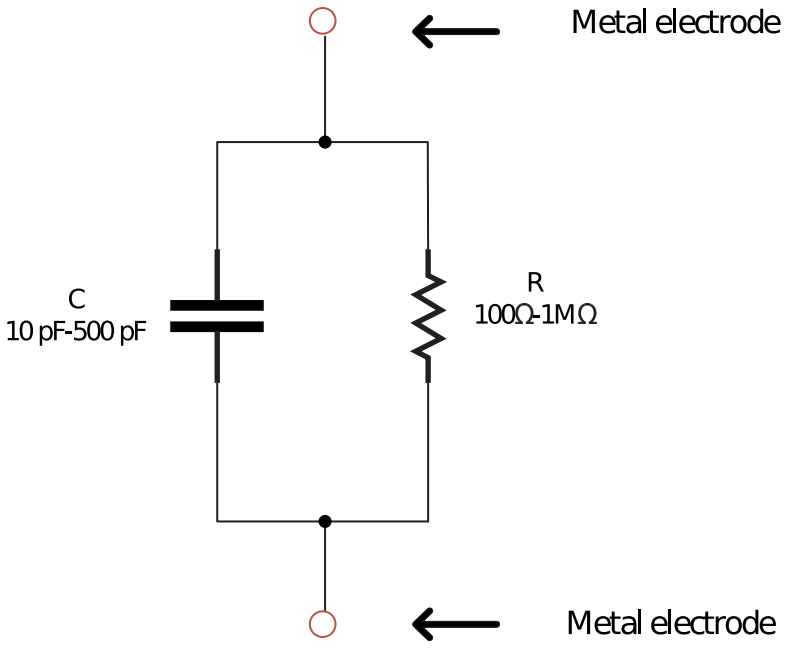

Fig. 14. The simplified equivalent circuit of the soil.
Source: Redrawn from Takimoto et al. (2023).

of the electrode and that of the load in the four-electrode system. This error can be minimised by following the bipolar injection method which is composed of two-phase controlled current sources in opposition (Bertemes-Filho, 2018). However, common-mode voltage will be generated at the inputs of the receive circuit due to any mismatch between the output current (Bertemes-Filho, 2018). Also, any other mismatch between drive electrode impedances will generate common-mode voltage (Bertemes-Filho, 2018).

3.3.2. Load stage measuring technique

The impedance of moist soil is represented by a parallel connection of capacitive and resistive components (Futagawa et al., 2018). This model is displayed in Fig. 14.

Here the resistance changes inversely with water and total ion contents, while the capacitance varies directly with the water content (Takimoto et al., 2023). In a multimodal system of sensors, the measurement of this resistance and capacitance are used to derive the water content and the total ion content in the soil (Takimoto et al., 2023). Combined information is presented by the resistance measurement. The capacitance component is utilised for assessing water content, while the total ion content can subsequently be derived (Takimoto et al., 2023). The soil's resistive and capacitive elements can be determined in the laboratory by employing the procedure outlined below and implementing the circuit depicted in Fig. 15 (Takimoto et al., 2023).

First, an electric current is injected into the soil. Then the output voltage will be measured resulting in a transient response characteristic (Fig. 16). The output response changes with the variations of the capacitance and the resistance of the soil. Then the following equations can be used to calculate the resistance and capacitance of the soil under test (Takimoto et al., 2023):

$$t_1 = -RCln(1 - \frac{2V_T}{R|+I|+V_T}) \tag{16}$$

$$t_2 = -RCln(1 - \frac{2V_T}{R|-I|+V_T}) \tag{17}$$

$$f = \frac{1}{t_1 + t_2} \tag{18}$$

where t_1 and t_2 represent the time needed to reach V_T and $-V_T$ (threshold voltage of the comparator) respectively, f is the frequency

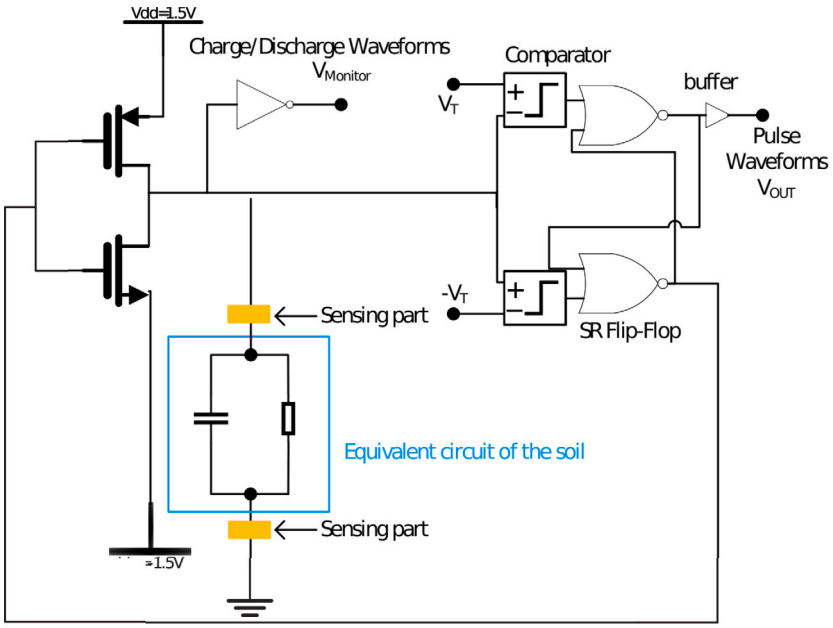

Fig. 15. Feedback type impedance measurement circuit for water content and electric conductivity sensor. *Source:* Redrawn from Takimoto et al. (2023).

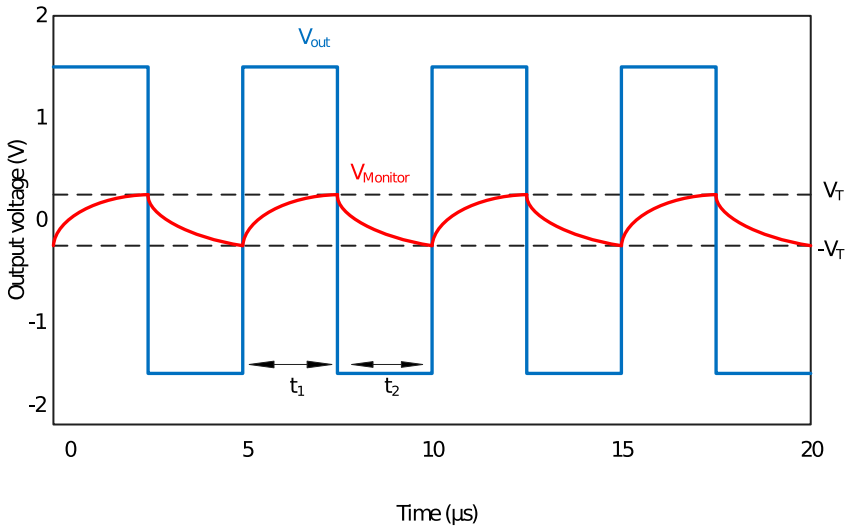

Fig. 16. Output waveform of the measurement circuit in Fig. 15.
Source: Redrawn from Takimoto et al. (2023).

of the square wave outputted by the measurement circuit, I is the injected current into the soil, R is the soil resistance, and C represents the capacitance of the soil (Takimoto et al., 2023).

Many different bulk material (soil) equivalent circuits have been developed by multiple researchers which are summarised in Fig. 17.

From Fig. 17, it can be observed that multiple equivalent models exist to represent a material.

(a) is the model previously discussed and it is usually used to represent pure electrolyte (Manjunath et al., 2023).

(b) was developed in 1992 by Gu et al. to represent the impedance of one layer of cement paste, and this model can be replicated multiple times depending on how many layers are under test; R_1 represents the summation of the bulk solid and liquid phase resistances, R_2 is the resistance of the solid–liquid interface, and C_2 is the capacitance of the solid–liquid interface (Gu et al., 1992).

(c) is the model developed by Song in 2000 to illustrate concrete also based on the different paths available in the soil; C_{SP} and R_{PP} represent the capacitance and the resistance at the discontinued point of the soil particle-pore path, C_{CSP} is the capacitance of the continuous pore path, and R_{CPP} is the resistance of the continuous pore path (Song, 2000).

(d) is a simplified equivalent circuit proposed by Song in 2000 and used by Han et al. in 2015 to represent a concrete material; R_1, R_2, C_1, and C_2 are the parameters of the electrochemical impedance spectroscopy spectrum, and these parameters are related to the parameters in Fig. 17(c) representing physical meanings for the soil microstructure (Han et al., 2015).

(e) represents the model developed by Dias in 1972 illustrating the interface effects with clays; C_{dl} is the double layer capacitance, Z_W represents the Warburg impedance, R represents a simple resistor describing the pure ohmic conduction of a free ionic path, R_{ct} is a resistor which value is proportional to the length of the average zone affected by the electrical double layer presence, and R_s is the resistance caused

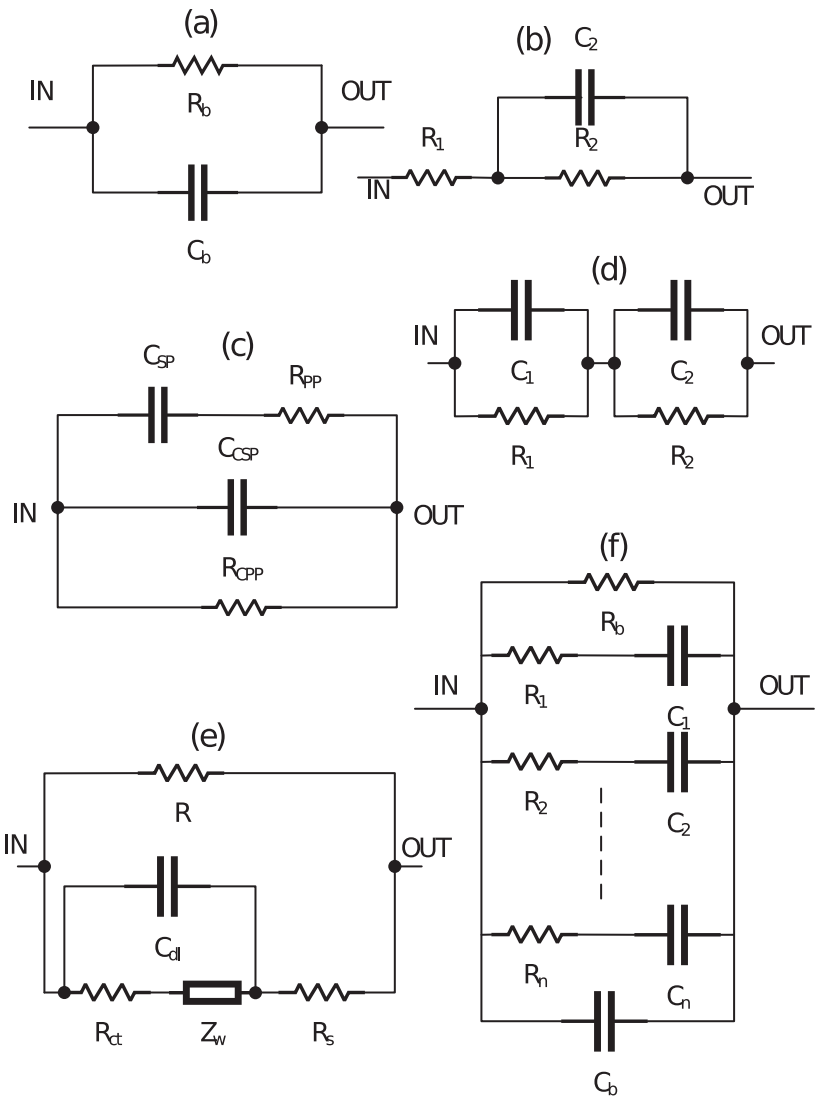

Fig. 17. Bulk material equivalent circuits.
Source: Redrawn from Manjunath et al. (2023).

by the polarisation associated with the metal-electrolyte interface (Dias, 2000).

(f) represents an R-C ladder network proposed in 1972 by Longmire and Longley; here R_b is the bulk medium DC resistance, C_b represents the capacitance at infinite frequency, $R_n - C_n$ series branches present the responses with different time constants to characterise the multiple relaxations with frequency, and the number n is determined from the order of the frequency response (Longmire and Longley, 1973).

From the preceding discussion concerning load representation, it is evident that there is no singular equivalent circuit for the soil's matrix, and researchers continue to adhere to these traditional representations. This increases the ambiguity about which model to follow, affecting the entire measuring system. In addition, the non-homogeneity characteristic of soil makes it very difficult to develop a unified soil electrical equivalent circuit.

3.3.3. Output stage measuring technique

This section discusses the output instrumentation for measuring soil impedance. When current is injected into the medium, a potential difference is generated across the load, which represents the output voltage to be measured. Typically, an instrumentation amplifier is used in the output stage of this type of instrument. However, alternative output circuits can also be employed, such as the one shown in Fig. 15. In this figure, the previously discussed procedure for identifying resistive and capacitive elements in the soil is also used to calculate its impedance. Changes in soil moisture or ion concentration affect soil impedance, which in turn alters the resistive and capacitive components, thereby modifying the output threshold voltages (Fig. 16). Thus, variations in impedance can be used to estimate soil moisture and ion content. Another example is shown in Fig. 18.

The circuit in Fig. 18 is used to amplify the signal, making it compatible with A/D converters. Electrode construction and positioning can affect measurements by inducing interference and noise (Bertemes-Filho, 2018). Additionally, artefacts and noise may result from electrode impedance and displacement (Bertemes-Filho, 2018). The instrumentation amplifier is being used for its key characteristics, for instance, high input impedance, high CMRR (common-mode rejection ratio), and low noise. However, instrumentation amplifiers are not perfect, and they may also amplify unwanted signals. Another issue with the output stage is related to gain. As mentioned earlier, signals need to be amplified to be measurable. However, the load introduces ambiguity, making it challenging to optimally tune the instrumentation amplifier. If the gain is high, the amplifier will go into saturation resulting in erroneous measurements. Moreover, if both the injected current

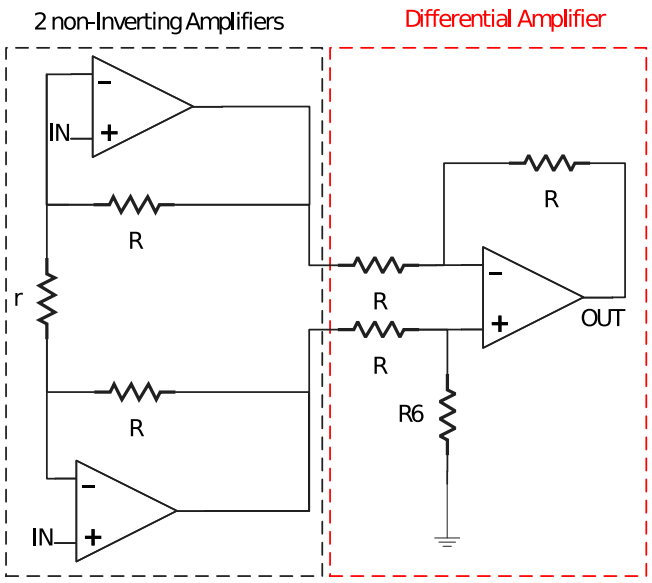

Fig. 18. Instrumentation amplifier used as the acquisition module.

and amplifier gain are too high, the outputs may saturate, producing incorrect results. Therefore, the output of the instrumentation amplifier is directly influenced by the magnitude of the injected current.

Many efforts have been made to resolve the aforementioned issues associated with electrical property measurement techniques but without success. Various solutions have been employed to reduce errors in these systems. One solution involves the use of a variable gain instrumentation amplifier, allowing the gain to adjust if saturation occurs. Another approach is implementing a feedback circuit to modify the injected current and prevent saturation. Additional solutions to these problems include applying multiple frequencies, as the resistive and capacitive elements of the soil vary with frequency. Manual calibration techniques, as previously mentioned, are also used to achieve accurate results, and this method is the most commonly employed. However, all these proposed solutions require significant time and labour, making the systems costly, highly power-consuming, and very complex.

4. Conclusion

Food insecurity and climate change are pressing issues that demand immediate attention. Unsustainable agriculture practices, such as excessive use of fertilisers, wasteful irrigation, and inadequate soil conditioning, are major contributors to these challenges. The reasons for following unsustainable agricultural practices include a lack of access to accurate technology and limited knowledge about these tools. Even when sensors and technology are employed, they often have significant inaccuracies. As a result, a large percentage of water wasted in irrigation can be attributed to not initially using technology, and when technology is available, it may not be advanced enough to provide accurate results that would help prevent excessive irrigation. This article investigates the causes of inaccuracies in soil moisture measurements and the factors influencing them. It explores the theory and instrumentation behind various techniques used to assess the electrical properties of soil.

An examination of the limitations of existing theories reveals that relying on current models often produces inaccurate results. This is primarily due to the presence of numerous assumptions inherent in these models when measuring soil electrical conductivity. On the other hand, the measurement techniques result in inaccurate results mainly caused by the effect of salinity inside the medium and the complexity of the soil matrix.

Consequently, it is evident from the preceding discussion that both theoretical frameworks and practical instruments exhibit errors and shortcomings. This underscores the link between flawed agricultural practices, such as wasteful irrigation and excessive fertiliser application, and the inadequacies in theory and instrumentation. Since every instrument relies on theory for calibration, the crucial question arises: how can we develop precise measurement techniques based on flawed theories? This question is of paramount importance for researchers addressing these pressing challenges with far-reaching consequences.

CRediT authorship contribution statement

Anthony Alhadchiti: Writing – review & editing, Writing – original draft, Methodology, Investigation, Conceptualization. **Bojan Nikolic:** Writing – review & editing, Methodology, Investigation, Conceptualization. **Panagiotis Ioakim:** Writing – review & editing, Supervision, Resources, Methodology, Investigation, Funding acquisition, Conceptualization. **Michael B. Powner:** Writing – review & editing, Supervision, Resources, Methodology, Investigation, Funding acquisition, Conceptualization. **Iasonas F. Triantis:** Writing – review & editing, Supervision, Resources, Methodology, Investigation, Funding acquisition, Conceptualization.

Declaration of competing interest

The authors declare the following financial interests/personal relationships which may be considered as potential competing interests: Anthony Alhadchiti reports financial support was provided by Delta-T Devices Ltd. Bojan Nikolic reports financial support was provided by Delta-T Devices Ltd. Panagiotis Ioakim reports a relationship with Delta-T Devices Ltd that includes: employment. If there are other authors, they declare that they have no known competing financial interests or personal relationships that could have appeared to influence the work reported in this paper.

Acknowledgements

We would like to thank City St George's, University of London and Delta-T Devices Ltd for jointly funding the work.

Data availability

No data was used for the research described in the article.

References

Abdullah, N.H.H., Kuan, N.W., Ibrahim, A., Ismail, B.N., Majid, M.R.A., Ramli, R., Mansor, N.S., Kuan, N.W., Ibrahim, A., Ismail, B.N., Majid, M.R.A., Ramli, R., Mansor, N.S., 2018. Determination of soil water content using time domain reflectometer (TDR) for clayey soil. AIP Conf. Proc. 2020 (20016), http://dx.doi.org/10.1063/1.5062642.

Abdulraheem, M.I., Zhang, W., Li, S., Moshayedi, A.J., Farooque, A.A., Hu, J., 2023. Advancement of remote sensing for soil measurements and applications: A comprehensive review. Sustainability 15, 15444. http://dx.doi.org/10.3390/SU152115444, URL: https://www.mdpi.com/2071-1050/15/21/15444/htmhttps://www.mdpi.com/2071-1050/15/21/15444, 2023 15, Page 15444.

Aboukila, E., Abdelaty, E., 2017. Assessment of saturated soil paste salinity from 1: 2.5 and 1: 5 soil–water extracts for coarse textured soils. Alexandria Sci. Exchange J. 38, 722–732.

Aboukila, E.F., Norton, J.B., 2017. Estimation of saturated soil paste salinity from soil–water extracts. Soil Sci. 182, 107–113.

Ahmed, W., Safdar, U., Ali, A., Haider, K., Tahir, N., Sajid, S., Ahmad, M., Nouman Khalid, M., Tayyab Sattar, M., 2022. Sustainable water use in agriculture: A review of worldwide research. Int. J. Agric. Biosci. 11, 246–250. http://dx.doi.org/10.47278/journal.ijab/2022.033.

Al-Moadhen, M.M., Clarke, B.G., Chen, X., 2022. Electrical conductivity of sand-clay mixtures. Environ. Geotech. http://dx.doi.org/10.1680/JENGE.21.00048/ASSET/IMAGES/SMALL/JENGEXXXX-0001-F12.GIF, URL: https://www.icevirtuallibrary.com/doi/10.1680/jenge.21.00048.

Aljoumani, B., Sànchez-Espigares, J.A., Cañameras, N., Josa, R., 2015. An advanced process for evaluating a linear dielectric constant–bulk electrical conductivity model using a capacitance sensor in field conditions. Hydrol. Sci. J. 60, 1828–1839. http://dx.doi.org/10.1080/02626667.2014.932053, URL: https://www.tandfonline.com/doi/abs/10.1080/02626667.2014.932053.

Aljoumani, B., Sanchez-Espigares, J.A., Wessolek, G., 2018. Estimating pore water electrical conductivity of sandy soil from time domain reflectometry records using a time-varying dynamic linear model. Sensors (Basel, Switz.) 18, http://dx.doi.org/10.3390/S18124403, URL: /pmc/articles/PMC6308429/ /pmc/articles/PMC6308429/?report=abstracthttps://www.ncbi.nlm.nih.gov/pmc/articles/PMC6308429/.

Alonge, T., Ojo, O., Adejumobi, A., 2019. Electrical conductivity based classification and mapping of salt affected soils in in kampe-omi irrigation scheme.

Balendonck, J., Tüzel, U., Oztekin, G.B., Tüzel, Y., 2021. Performance evaluation of the AquaTag, a prototype near-field RF-based soil moisture sensor. In: 2021 13th International Conference on Electromagnetic Wave Interaction with Water and Moist Substances. ISEMA 2021, http://dx.doi.org/10.1109/ISEMA49699.2021.9508292.

Bangi, U.K., Bachuwar, V.D., Park, H.H., 2021. Zirconia coatings as efficient soil moisture sensors for water irrigation. IEEE Sensors J. 21, 21205–21211. http://dx.doi.org/10.1109/JSEN.2021.3102973.

Bañón, S., Álvarez, S., Bañón, D., Ortuño, M.F., Sánchez-Blanco, M.J., 2021. Assessment of soil salinity indexes using electrical conductivity sensors. Sci. Hort. 285, 110171. http://dx.doi.org/10.1016/J.SCIENTA.2021.110171.

Bellosta-Diest, A., Campo-Bescós, M., Zapatería-Miranda, J., Casalí, J., Arregui, L.M., 2022. Evaluation of nitrate soil probes for a more sustainable agriculture. Sensors (Basel, Switz.) 22, http://dx.doi.org/10.3390/S22239288, URL: /pmc/articles/PMC9739946//pmc/articles/PMC9739946/?report=abstracthttps://www.ncbi.nlm.nih.gov/pmc/articles/PMC9739946/.

Bera, T.K., 2014. Bioelectrical impedance methods for noninvasive health monitoring: A review. J. Med. Eng. 2014, 1–28. http://dx.doi.org/10.1155/2014/381251, URL: https://pubmed.ncbi.nlm.nih.gov/27006932/.

Bertemes-Filho, P., 2018. Electrical impedance spectroscopy. Bioimpedance Biomed. Appl. Res. 5–27. http://dx.doi.org/10.1007/978-3-319-74388-2{_}2/FIGURES/16, URL: https://link.springer.com/chapter/10.1007/978-3-319-74388-2_2.

Biswas, A., Yin, S., Tursunniyaz, M., Karamimohammadi, N., Huang, J., Andrews, J., 2022. Geometrical optimization of printed interdigitated electrode sensors to improve soil moisture sensitivity. IEEE Sensors J. 22, 19162–19169. http://dx.doi.org/10.1109/JSEN.2022.3200008.

Bristow, N., Rengaraj, S., Chadwick, D.R., Kettle, J., Jones, D.L., 2022. Development of a LoRaWAN IoT node with ion-selective electrode soil nitrate sensors for precision agriculture. Sensors 22, http://dx.doi.org/10.3390/S22239100/S1, URL: /pmc/articles/PMC9739143//pmc/articles/PMC9739143/?report=abstrachttps://www.ncbi.nlm.nih.gov/pmc/articles/PMC9739143/.

Chan, J., 2018. Salinity / electrical conductivity (ec). URL: https://soilsensor.com/articles/salinity-electrical-conductivity-ec/.

Chan, J., 2019. Time domain reflectometry (tdr). URL: https://soilsensor.com/articles/time-domain-reflectometry-tdr/#:~:text=TDR%20sensors%20should%20not%20be%20used%20in%20high,is%20attenuated%20beyond%20the%20length%20of%20the%20rod.

Chi, C.M., Wang, Z.C., 2010. Characterizing salt-affected soils of songnen plain using saturated paste and 1: 5 soil-to-water extraction methods. Arid. Land Res. Manag. 24, 1–11.

Choo, H., Park, J., Do, T.T., Lee, C., 2022. Estimating the electrical conductivity of clayey soils with varying mineralogy using the index properties of soils. Appl. Clay Sci. 217, 106388. http://dx.doi.org/10.1016/J.CLAY.2021.106388.

Corwin, D.L., Scudiero, E., 2020. Field-scale apparent soil electrical conductivity. Soil Sci. Am. J. 84, 1405–1441. http://dx.doi.org/10.1002/SAJ2.20153, URL: https://onlinelibrary.wiley.com/doi/full/10.1002/saj2.20153https://onlinelibrary.wiley.com/doi/abs/10.1002/saj2.20153https://acsess.onlinelibrary.wiley.com/doi/10.1002/saj2.20153.

Da Costa Junior, R.L., Rodrigues, E.O., Antayhua, R.A.R., 2021. Coplanar capacitor probes design for a moisture soil sensor operating at high frequencies. In: INSCIT 2021-5th International Symposium on Instrumentation Systems, Circuits and Transducers. http://dx.doi.org/10.1109/INSCIT49950.2021.9557243.

Datsios, Z.G., Mikropoulos, P.N., 2019. Characterization of the frequency dependence of the electrical properties of sandy soil with variable grain size and water content. IEEE Trans. Dielectr. Electr. Insul. 26, 904–912. http://dx.doi.org/10.1109/TDEI.2018.007864.

Dey, A., Sharma, C., Sarma, U., 2022. Fringing field capacitive sensor: A study of different configurations for soil moisture measurement. In: MESIICON 2022 - International Interdisciplinary Conference on Mathematics, Engineering and Science, Proceedings. http://dx.doi.org/10.1109/MESIICON55227.2022.10093331.

Dias, C.A., 2000. Developments in a model to describe low-frequency electrical polarization of rocks. Geophys. 65, 437–451. http://dx.doi.org/10.1190/1.1444738, URL: https://www.researchgate.net/publication/260541480_Developments_in_a_model_to_describe_low-frequency_electrical_polarization_of_rocks.

Duncombe, J., 2021. Index suggests that half of nitrogen applied to crops is lost. URL: https://eos.org/articles/index-suggests-that-half-of-nitrogen-applied-to-crops-is-lost.

Fan, W., Kam, K.A., Zhao, H., Culligan, P.J., Kymissis, I., 2022. An optical soil sensor for NPK nutrient detection in smart cities. In: 2022 18th International Conference on Intelligent Environments, IE 2022 - Proceedings. http://dx.doi.org/10.1109/IE54923.2022.9826759.

Faruque, M.J., Mojid, M.A., Delwar Hossain, A.S.M., 2006. Effects of soil texture and water on bulk soil electrical conductivity. J. Bangladesh Agric. Univ. 4, 381–389. http://dx.doi.org/10.22004/AG.ECON.276570, URL: https://ageconsearch.umn.edu/record/276570.

publisherCreate a flipbook, D.D.t., 2008. Ec-tm, ech2o-te manual. URL: https://issuu.com/decaweb/docs/manualech2o-te_ec-tm.

Futagawa, M., Ogasahara, S., Ito, T., Komatsu, M., Fuwa, Y., Hirano, H., Akita, I., Kusano, K., Watanabe, M., 2018. Fabrication of a low leakage current type impedance sensor with shielding structures to detect a low water content of soil for slope failure prognostics. Sensors Actuators A: Phys. 271, 383–388. http://dx.doi.org/10.1016/J.SNA.2017.12.022.

Geyer, M., Karastergiou, A., 2016. The frequency dependence of scattering imprints on pulsar observations. Mon. Not. R. Astron. Soc. 462, 2587–2602. http://dx.doi.org/10.1093/MNRAS/STW1724.

Gharaibeh, M.A., Albalasmeh, A.A., Hanandeh, A.El., 2021. Estimation of saturated paste electrical conductivity using three modelling approaches: Traditional dilution extracts; saturation percentage and artificial neural networks. CATENA 200, 105141. http://dx.doi.org/10.1016/J.CATENA.2020.105141.

Gong, L., 2022. Soil electrical conductivity(ec): What's it, why important, how to measure & more. URL: https://www.seeedstudio.com/blog/2022/07/15/soil-electrical-conductivity/.

González-Teruel, J.D., Jones, S.B., Soto-Valles, F., Torres-Sánchez, R., Lebron, I., Friedman, S.P., Robinson, D.A., 2020. Dielectric spectroscopy and application of mixing models describing dielectric dispersion in clay minerals and clayey soils. Sensors (Basel, Switz.) 20, 1–18. http://dx.doi.org/10.3390/S20226678, URL: /pmc/articles/PMC7700415//pmc/articles/PMC7700415/?report=abstracthttps://www.ncbi.nlm.nih.gov/pmc/articles/PMC7700415/.

González-Teruel, J.D., Ruiz-Abellon, M.C., Blanco, V., Blaya-Ros, P.J., Domingo, R., Torres-Sánchez, R., 2022. Prediction of water stress episodes in fruit trees based on soil and weather time series data. Agronomy 12, 1422. http://dx.doi.org/10.3390/AGRONOMY12061422, URL: https://www.mdpi.com/2073-4395/12/6/1422/htmhttps://www.mdpi.com/2073-4395/12/6/1422, 2022 12, 1422.

González-Teruel, J.D., Torres-Sánchez, P.J., Toledo-Moreo, A.B., Jiménez-Buendía, M., Soto-Valles, F., 2019. Design and calibration of a low-cost SDI-12 soil moisture sensor. Sensors (Basel, Switz.) 19, http://dx.doi.org/10.3390/S19030491, URL: /pmc/articles/PMC9739143//pmc/articles/PMC9739143/?report= abstract.

González-Teruel J.D. Jones, S.B., Robinson, D.A., Giménez-Gallego, R., Torres-Sánchez, R., 2022a. Measurement of the broadband complex permittivity of soils in the frequency domain with a low-cost vector network analyzer and an open-ended coaxial probe. Comput. Electron. Agric. 195, 106847. http://dx.doi.org/10.1016/J.COMPAG.2022.106847.

Goodchild, M.S., 2023. An investigation into the impact of soil particle conductivity and percolation threshold on the hilhorst model to estimate pore water conductivity in soils. Soil Sci. Am. J. 87, 1221–1228. http://dx.doi.org/10.1002/SAJ2.20561, URL: https://onlinelibrary.wiley.com/doi/full/10.1002/saj2.20561https://onlinelibrary.wiley.com/doi/abs/10.1002/saj2.20561 https://acsess.onlinelibrary.wiley.com/doi/10.1002/saj2.20561.

Goswami, M.P., Montazer, B., Sarma, U., 2019. Design and characterization of a fringing field capacitive soil moisture sensor. IEEE Trans. Instrum. Meas. 68, 913–922. http://dx.doi.org/10.1109/TIM.2018.2855538.

Gu, P., Xie, P., Beaudoin, J.J., Brousseau, R., 1992. A.C. impedance spectroscopy (i): A new equivalent circuit model for hydrated portland cement paste. Cem. Concr. Res. 22, 833–840. http://dx.doi.org/10.1016/0008-8846(92)90107-7.

Hamed, Y., Persson, M., Berndtsson, R., 2003. Soil solution electrical conductivity measurements using different dielectric techniques. Soil Sci. Am. J. 67, 1071–1078. http://dx.doi.org/10.2136/SSSAJ2003.1071.

Han, P.j., Zhang, Y.f., Chen, F.Y., Bai, X.h., 2015. Interpretation of electrochemical impedance spectroscopy (EIS) circuit model for soils. J. Central South Univ. 22, 4318–4328. http://dx.doi.org/10.1007/S11771-015-2980-1/METRICS, URL: https://link.springer.com/article/10.1007/s11771-015-2980-1.

Hayley, K., Bentley, L.R., Gharibi, M., Nightingale, M., 2007. Low temperature dependence of electrical resistivity: Implications for near surface geophysical monitoring. Geophys. Res. Lett. 34, 18402, URL: https://onlinelibrary.wiley.com/doi/full/10.1029/2007GL031124https://onlinelibrary.wiley.com/doi/abs/10.1029/2007GL031124https://agupubs.onlinelibrary.wiley.com/doi/10.1029/2007GL031124.

He, Y., DeSutter, T., Hopkins, D., Jia, X., Wysocki, D.A., 2013. Predicting ece of the saturated paste extract from value of ec1: 5. Can. J. Soil Sci. 93, 585–594.

Herrero, J., Pérez-Coveta, O., 2005. Soil salinity changes over 24 years in a mediterranean irrigated district. Geoderma 125, 287–308.

Hilhorst, M.A., 2000. A pore water conductivity sensor. Soil Sci. Am. J. 64, 1922–1925. http://dx.doi.org/10.2136/SSSAJ2000.6461922X, URL: https://onlinelibrary.wiley.com/doi/full/10.2136/sssaj2000.6461922xhttps://onlinelibrary.wiley.com/doi/abs/10.2136/sssaj2000.6461922xhttps://acsess.onlinelibrary.wiley.com/doi/10.2136/sssaj2000.6461922x.

Hillel, D.E., 1981. Soil colloids: The role of electric double layer forces.

Hossain, M.S., Rahman, G.K.M.M., Solaiman, A.R.M., Alam, M.S., Rahman, M.M., Mia, M.A.B., 2020. Estimating electrical conductivity for soil salinity monitoring using various soil-water ratios depending on soil texture. Commun. Soil Sci. Plant Anal. 51, 635–644. http://dx.doi.org/10.1080/00103624.2020.1729378, URL: https://www.tandfonline.com/doi/full/10.1080/00103624.2020.1729378.

Iranmanesh, M., Sadeghi, H., 2019. The effect of soil organic matter, electrical conductivity and acidity on the soil's carbon sequestration ability via two species of tamarisk (tamarix spp.). Environ. Prog. Sustain. Energy 38, 13230. http://dx.doi.org/10.1002/EP.13230, URL: https://onlinelibrary.wiley.com/doi/full/10.1002/ep.13230https://onlinelibrary.wiley.com/doi/abs/10.1002/ep.13230https://aiche.onlinelibrary.wiley.com/doi/10.1002/ep.13230.

Ismayilov, A.I., Mamedov, A.I., Fujimaki, H., Tsunekawa, A., Levy, G.J., 2021. Soil salinity type effects on the relationship between the electrical conductivity and salt content for 1:5 soil-to-water extract. Sustain. 13, 3395. http://dx.doi.org/10.3390/SU13063395, URL: https://www.mdpi.com/2071-1050/13/6/3395/htmhttps://www.mdpi.com/2071-1050/13/6/3395, 2021 13, Page 3395.

Jin, P.H., Yang, H.I., IN, Seo, B.S., Dong-hwan, L., Kim, H., Choi, W.J., 2019. Assessment of electrical conductivity of saturated soil paste from 1:5 soil-water extracts for reclaimed tideland soils in south-Western Coastal Area of Korea. Korean J. Environ. Agric. 38, 69–75.

John, J., Palaparthy, V.S., Dethe, A., Baghini, M.S., 2021. A temperature compensated soil specific calibration approach for frequency domain soil moisture sensors for in-situ agricultural applications. In: 2021 IEEE Sensors Applications Symposium, SAS 2021 - Proceedings. http://dx.doi.org/10.1109/SAS51076.2021.9530177.

Kadan-Jamal, K., Sophocleous, M., Jog, A., Desagani, D., Teig-Sussholz, O., Georgiou, J., Avni, A., Shacham-Diamand, Y., 2020. Electrical impedance spectroscopy of plant cells in aqueous biological buffer solutions and their modelling using a unified electrical equivalent circuit over a wide frequency range: 4Hz to 20 GHz. Biosens. Bioelectron. 168, 112485. http://dx.doi.org/10.1016/J.BIOS.2020.112485.

Kamewada, K., Ooshima, M., 2024. A proposed method for determining potentially environmentally available trace metals in paddy soil. Soil Sci. Plant Nutr. 70, 123–128. http://dx.doi.org/10.1080/00380768.2024.2304752, URL: https://www.tandfonline.com/doi/abs/10.1080/00380768.2024.2304752.

Kargas, G., Chatzigiakoumis, I., Kollias, A., Spiliotis, D., Kerkides, P., 2018a. An investigation of the relationship between the electrical conductivity of the soil saturated paste extract ECe with the respective values of the mass soil/water ratios 1:1 and 1:5 (EC1:1 and EC1:5). Proceedings 2, 661. http://dx.doi.org/10.3390/PROCEEDINGS2110661, URL: https://www.mdpi.com/2504-3900/2/11/661/htmhttps://www.mdpi.com/2504-3900/2/11/661, 2018 2, Page 661.

Kargas, G., Chatzigiakoumis, I., Kollias, A., Spiliotis, D., Massas, I., Kerkides, P., 2018b. Soil salinity assessment using saturated paste and mass soil: water 1: 1 and 1: 5 ratios extracts. Water 10, 1589.

Kargas, G., Londra, P., Sgoubopoulou, A., 2020. Comparison of soil ec values from methods based on 1: 1 and 1: 5 soil to water ratios and ece from saturated paste extract based method. Water 12, 1010.

Khorsandi, F., Yazdi, F.A., 2011. Estimation of saturated paste extracts' electrical conductivity from 1: 5 soil/water suspension and gypsum. Commun. Soil Sci. Plant Anal. 42, 315–321.

Klaustermeier, A., Tomlinson, H., Daigh, A.L., Limb, R., DeSutter, T., Sedivec, K., 2016. Comparison of soil-to-water suspension ratios for determining electrical conductivity of oil-productionwater-contaminated soils. Can. J. Soil Sci. 96, 233–243. http://dx.doi.org/10.1139/CJSS-2015-0097/ASSET/IMAGES/CJSS-2015-0097TAB4.GIF, URL: https://cdnsciencepub.com/doi/10.1139/cjss-2015-0097.

Ko, H., Choo, H., Ji, K., 2023. Effect of temperature on electrical conductivity of soils – role of surface conduction. Eng. Geol. 321, 107147. http://dx.doi.org/10.1016/J.ENGGEO.2023.107147.

Kumar, M.S., Chandra, T.R., Kumar, D.P., Manikandan, M.S., 2016. Monitoring moisture of soil using low cost homemade soil moisture sensor and arduino UNO. In: ICACCS 2016-3rd International Conference on Advanced Computing and Communication Systems: Bringing To the Table, Futuristic Technologies from Arround the Globe. http://dx.doi.org/10.1109/ICACCS.2016.7586312.

Leksungnoen, N., Andriyas, T., Andriyas, S., 2018. Ece prediction from ec1: 5 in inland salt-affected soils collected from khorat and sakhon nakhon basins, thailand. Commun. Soil Sci. Plant Anal. 49, 2627–2637.

Lin, C.P., Chung, C.C., Chang, Y.C., Chang, T.S., 2010. Development of sediment monitoring during heavy rainfalls. Adv. Environ. Geotech. 531–536. http://dx.doi.org/10.1007/978-3-642-04460-1{_}50, URL: https://www.researchgate.net/publication/301196361_Development_of_Sediment_Monitoring_During_Heavy_Rainfalls.

Liu, S., Sun, A., Li, S., Zeng, Q., Wu, H., 2020. Analysis and modeling of the complex dielectric constant of bound water with application in soil microwave remote sensing. Remote. Sens. 12, 3544.

Loewer, M., Igel, J., Wagner, N., 2014. Frequency-dependent attenuation analysis in soils using broadband dielectric spectroscopy and TDR. In: Proceedings of the 15th International Conference on Ground Penetrating Radar. GPR 2014, 2014, pp. 208–213. http://dx.doi.org/10.1109/ICGPR.2014.6970415.

Longmire, C., Longley, H., 1973. Time domain treatment of media with frequency-dependent electrical parameters.

Ma, X., Bifano, L., Fischerauer, G., 2023. Evaluation of electrical impedance spectra by long short-term memory to estimate nitrate concentrations in soil. Sensors (Basel, Switz.) 23, http://dx.doi.org/10.3390/S23042172, URL: /pmc/articles/PMC9964299//pmc/articles/PMC9964299/?report=abstracthttps://www.ncbi.nlm.nih.gov/pmc/articles/PMC9964299/.

Manjunath, A.D.B., Harid, N., Griffiths, H., Nogueira, R.P., Noyanbayev, N., Haddad, A., Ramanujam, S., 2023. Equivalent circuit models for soils and aqueous solutions under 2-terminal test configuration. IEEE Trans. Electromagn. Compat. 65, 225–234. http://dx.doi.org/10.1109/TEMC.2022.3216813.

Menne, D., Hübner, D., Willenbacher, N., 2021. A robust soil water potential sensor with high sensitivity and broad measuring range. In: 2021 13th International Conference on Electromagnetic Wave Interaction with Water and Moist Substances. ISEMA 2021, http://dx.doi.org/10.1109/ISEMA49699.2021.9508320.

Minet, J., Lambot, S., Delaide, G., Huisman, J., Vereecken, H., Vanclooster, M., 2010. A generalized frequency domain reflectometry modeling technique for soil electrical properties determination. Vadose Zone J. 9, 1063–1072. http://dx.doi.org/10.2136/VZJ2010.0004, URL: https://onlinelibrary.wiley.com/doi/full/10.2136/vzj2010.0004https://onlinelibrary.wiley.com/doi/abs/10.2136/vzj2010.0004https://acsess.onlinelibrary.wiley.com/doi/10.2136/vzj2010.0004.

Mojid, M.A., 2011. Diffuse double layer (DDL). Encycl. Earth Sci. Ser. Part 4, 213–214. http://dx.doi.org/10.1007/978-90-481-3585-1{_}41, URL: https://link.springer.com/referenceworkentry/10.1007/978-90-481-3585-1_41.

Morais, F., Carvalhaes-Dias, P., Duarte, L., Costa, E., Ferreira, A., Dias, J.S., Palma, A.J., 2019. Fringing field capacitive smart sensor based on PCB technology for measuring water content in paper pulp. http://dx.doi.org/10.1155/2020/3905804.

Moreno-Maroto, J.M., Alonso-Azcárate, J., 2018. What is clay? A new definition of clay based on plasticity and its impact on the most widespread soil classification systems. Appl. Clay Sci. 161, 57–63. http://dx.doi.org/10.1016/J.CLAY.2018.04.011.

Moriana, A., Pérez-López, D., Prieto, M.H., Ramírez-Santa-Pau, M., Pérez-Rodriguez, J.M., 2012. Midday stem water potential as a useful tool for estimating irrigation requirements in olive trees. Agricult. Water. Manag. 112, 43–54. http://dx.doi.org/10.1016/J.AGWAT.2012.06.003.

Mukhlisin, M., Astuti, H.W., Wardihani, E.D., Matlan, S.J., 2021. Arab. J. Geosci. 14, 1–34. http://dx.doi.org/10.1007/S12517-021-08263-0, URL: https://link.springer.com/article/10.1007/s12517-021-08263-0, 2021 14:19.

Nagahage, E.A.A.D., Nagahage, I.S.P., Fujino, T., 2019. Calibration and validation of a low-cost capacitive moisture sensor to integrate the automated soil moisture monitoring system. Agriculture 9 (141), http://dx.doi.org/10.3390/AGRICULTURE9070141, URL: https://www.mdpi.com/2077-0472/9/7/141/htmhttps://www.mdpi.com/2077-0472/9/7/141, 2019 9, Page 141.

Ohkawara, S., Miura, K., Hirano, H., Ota, S., Futagawa, M., 2022. Evaluation of a hydrogen signal detection method using a compact NMR sensor for the measurement of ion concentrations in culture medium. Electron. Commun. Japan 105, e12346. http://dx.doi.org/10.1002/ECJ.12346, URL: https://onlinelibrary.wiley.com/doi/full/10.1002/ecj.12346https://onlinelibrary.wiley.com/doi/abs/10.1002/ecj.12346https://onlinelibrary.wiley.com/doi/10.1002/ecj.12346.

Ozcan, H., Ekinci, H., Yigini, Y., Yuksel, O., 2006. Comparison of four soil salinity extraction methods. In: Proceedings of 18th International Soil Meeting on Soil Sustaining Life on Earth, Managing Soil and Technology. pp. 697–703.

Pieris, T.P., Chathuranga, K.V., 2020. Design and evaluation of a capacitive sensor for real time monitoring of gravimetric moisture content in soil. In: Proceedings of ICITR 2020-5th International Conference on Information Technology Research: Towards the New Digital Enlightenment. http://dx.doi.org/10.1109/ICITR51448.2020.9310793.

Placidi, P., Delle Vergini, C.V., Papini, N., Ciancabilla, E., Cecconi, M., Scorzoni, A., 2023. Soil water content sensor in the IoT precision agriculture. In: Proceedings of IEEE Sensors. http://dx.doi.org/10.1109/SENSORS56945.2023.10324958.

Popov, I., Cheng, S., Sokolov, A.P., 2022. Broadband dielectric spectroscopy and its application in polymeric materials. Macromol. Eng. 1–39. http://dx.doi.org/10.1002/9783527815562.MME0059, URL: https://onlinelibrary.wiley.com/doi/full/10.1002/9783527815562.mme0059https://onlinelibrary.wiley.com/doi/abs/10.1002/9783527815562.mme0059https://onlinelibrary.wiley.com/doi/10.1002/9783527815562.mme0059.

Quan, Z., Zhang, X., Fang, Y., Davidson, E.A., 2021. Different quantification approaches for nitrogen use efficiency lead to divergent estimates with varying advantages. Nat. Food 2, 241–245. http://dx.doi.org/10.1038/s43016-021-00263-3, URL: https://www.nature.com/articles/s43016-021-00263-3, 2021 2:4.

Regalado, C.M., Muñz Carpena, A.R., Hernández Moreno, J.M., 2003. Time domain reflectometry models as a tool to understand the dielectric response of volcanic soils. Geoderma 117, 313–330. http://dx.doi.org/10.1016/S0016-7061(03)00131-9.

Revil, A., Ward, P., Bellarby, A., Binley, P., Constable, D.N., Voxman, A., 2016. Modelling the spectral induced polarization response of water-saturated sands in the intermediate frequency range (10^2 – 10^5 hz) using mechanistic and empirical approaches. Geophys. J. Int. 207, 1303–1318.

Rhoades, J., 1982. Soluble salts. pp. 167–179. http://dx.doi.org/10.2134/AGRONMONOGR9.2.2ED.C10.

Richards, L.A., 1954. Diagnosis and Improvement of Saline and Alkali Soils, vol. 60, US Government Printing Office.

Robertson, P., VanderWulp, S., 2024. Soil moisture protocol. Kellogg biological station long-term ecological research (KBS LTER). URL: https://lter.kbs.msu.edu/protocols/24. (Accessed 18 March 2025).

Sanchez, J., Dahal, A., Zesiger, C., Goel, R., Young, D., Roundy, S., 2021. Design and characterization of a low-power moisture sensor from commercially available electronics. In: Proceedings of IEEE Sensors, 2021-October. http://dx.doi.org/10.1109/SENSORS47087.2021.9639573.

Sanket, R.J., Baviskar, A., Ahire, S.S., Mapare, S.V., 2018. Development of a low cost nitrate detection soil sensor. In: Proceedings of the 2017 International Conference on Wireless Communications, Signal Processing and Networking, WiSPNET 2017, 2018-January. pp. 1272–1275. http://dx.doi.org/10.1109/WISPNET.2017.8299968.

Teixeira Ricardo Correia dos Santos, J., Teixeira, J., Correia dos Santos, R., 2021. Exploring the applicability of low-cost capacitive and resistive water content sensors on compacted soils capacitive sensors DC direct current FBG fibre bragg grating FDR frequency domain reflectometry R1, R2, R3 resistive sensors TDT time domain transmission TDR time domain reflectometry. Geotech. Geol. Eng. 39, 2969–2983. http://dx.doi.org/10.1007/s10706-020-01672-0.

Seo, B.S., Jeong, Y.J., Baek, N.R., Park, H.J., Yang, H.I., Park, S.I., Choi, W.J., 2022. Soil texture affects the conversion factor of electrical conductivity from 1:5 soil–water to saturated paste extracts. Pedosphere 32, 905–915. http://dx.doi.org/10.1016/J.PEDSPH.2022.06.023.

Shen, S., Guo, P., Wu, J., Ding, Y., Chen, F., Meng, F., Xu, Z., 2019. Optimized inside-out magnetic resonance probe for soil moisture measuring in situ. J. Magn. Reson. 307, 106565. http://dx.doi.org/10.1016/J.JMR.2019.07.052.

Shigemasu, R., Teraoka, Y., Ota, S., Hirano, H., Yasutomi, K., Kawahito, S., Futagawa, M., 2022. Development of a current injection—Type impedance measurement system for monitoring soil water content and ion concentration. Sensors (Basel, Switz.) 22, http://dx.doi.org/10.3390/S22093509, URL: /pmc/articles/PMC9106015//pmc/articles/PMC9106015/?report=abstracthttps://www.ncbi.nlm.nih.gov/pmc/articles/PMC9106015.

Shu, X., He, J., Zhou, Z., Xia, L., Hu, Y., Zhang, Y., Zhang, Y., Luo, Y., Chu, H., Liu, W., Yuan, S., Gao, X., Wang, C., 2022. Organic amendments enhance soil microbial diversity, microbial functionality and crop yields: A meta-analysis. Sci. Total Environ. 829, 154627. http://dx.doi.org/10.1016/J.SCITOTENV.2022.154627.

Siontorou, C.G., Georgopoulos, K.N., 2016. A biosensor platform for soil management: the case of nitrites. J. Clean. Prod. 111, 133–142. http://dx.doi.org/10.1016/J.JCLEPRO.2015.07.038.

Song, G., 2000. Equivalent circuit model for AC electrochemical impedance spectroscopy of concrete. Cem. Concr. Res. 30, 1723–1730. http://dx.doi.org/10.1016/S0008-8846(00)00400-2.

Sonmez, S., Buyuktas, D., Okturen, F., Citak, S., 2008. Assessment of different soil to water ratios (1:1, 1:2.5, 1:5) in soil salinity studies. Geoderma 144, 361–369. http://dx.doi.org/10.1016/J.GEODERMA.2007.12.005.

Souza, G., De Faria, B.T., Alves, R.Gomes., Lima, F., Aquino, P.T., Soininen, J.P., 2020. Calibration equation and field test of a capacitive soil moisture sensor. In: 2020 IEEE International Workshop on Metrology for Agriculture and Forestry, MetroAgriFor 2020 - Proceedings. pp. 180–184. http://dx.doi.org/10.1109/METROAGRIFOR50201.2020.9277634.

Spikic, D., Svraka, M., Vasic, D., 2022. Contactless sensing of soil electrical conductivity using high frequency electromagnetic induction. In: Proceedings of IEEE Sensors, 2022-October. http://dx.doi.org/10.1109/SENSORS52175.2022.9967093.

Spiteri, K., Sacco, A.T., 2024. Estimating the electrical conductivity of a saturated soil paste extract (ECe) from 1:1(EC1:1), 1:2(EC1:2) and 1:5(EC1:5) soil:water suspension ratios, in calcareous soils from the mediterranean islands of malta. Commun. Soil Sci. Plant Anal. 55, 1302–1312. http://dx.doi.org/10.1080/00103624.2024.2304636, URL: https://www.tandfonline.com/doi/abs/10.1080/00103624.2024.2304636.

Sriphanthaboot, W., Saengow, T., Kamonkusonman, K., Phunthawornwong, M., Simmanee, P., Silapunt, R., 2021. Smart multi-level soil moisture sensing system. In: 2021 2nd International Symposium on Instrumentation, Control, Artificial Intelligence, and Robotics. ICA-SYMP 2021, http://dx.doi.org/10.1109/ICA-SYMP50206.2021.9358450.

Surya, S.G., Yuvaraja, S., Salama, K.N., Shojaei Baghini, M., Palaparthy, V.S., 2019. Molybdenum trioxide (MoO3) capacitive soil moisture microsensor for in-situ agriculture applications: Measurement studies and temperature effects. In: Proceedings of IEEE Sensors, 2019-October. http://dx.doi.org/10.1109/SENSORS43011.2019.8956768.

Susha Lekshmi, S.U., Singh, D.N., Shojaei Baghini, M., 2014. A critical review of soil moisture measurement. Measurement 54, 92–105. http://dx.doi.org/10.1016/J.MEASUREMENT.2014.04.007.

Takimoto, S., Shigemasu, R., Fujisono, M., Ota, S., Futagawa, M., 2023. Development of frequency measurement circuit for soil moisture content and electric conductivity measurement system with detection of soil transient response characteristics for on-site measurement. Electron. Commun. Japan 106, http://dx.doi.org/10.1002/ECJ.12415.

Tomar, M., Patidar, T., 2019. Development of a low cost soil moisture sensor. In: Proceedings - International Conference on Vision Towards Emerging Trends in Communication and Networking. ViTECoN 2019, http://dx.doi.org/10.1109/VITECON.2019.8899399.

Topp, G.C., 1980. Electromagnetic permittivity of minerals and rocks at microwave frequencies. Soil Sci. Am. J. 44, 165–171.

Trigona, C., 2020. Feasibility of a soil-based sensor for measurement of temperature. In: Proceedings of the 17th International Multi-Conference on Systems, Signals and Devices. SSD 2020, pp. 1155–1158. http://dx.doi.org/10.1109/SSD49366.2020.9364110.

USDA-NRCS, 2024. Soil health – electrical conductivity. https://www.nrcs.usda.gov/sites/default/files/2022-10/Soil%20Electrical%20Conductivity%20Educators.pdf. (Accessed 08 February 2024).

Visconti, F., de Paz, J.M., 2012. Prediction of the soil saturated paste extract salinity from extractable ions, cation exchange capacity, and anion exclusion. Soil Res. 50, 536–550.

Walczak, A., Lipiński, G., 2021. Application of the TDR sensor and the parameters of injection irrigation for the estimation of soil evaporation intensity. Sensors 21 (2309), http://dx.doi.org/10.3390/S21072309, URL: https://www.mdpi.com/1424-8220/21/7/2309/htmhttps://www.mdpi.com/1424-8220/21/7/2309, 2021 21, Page 2309.

Wijaya, K., Nishimura, T., Kato, M., 2003. Estimation of dry bulk density of soil using amplitude domain reflectometry probe. J. Jpn. Soc. Soil Phys. 95, 63–73. http://dx.doi.org/10.34467/jssoilphysics.95.0{_}63, URL: https://www.jstage.jst.go.jp/article/jssoilphysics/95/0/95_63/_article/-char/en.

Xu, Y., Chen, Q., Hu, D., Li, B., Tang, H., 2022. Modeling and testing of fringe-field capacitive moisture sensor under Certain Electrode Area. IEEE Trans. Instrum. Meas. 71, http://dx.doi.org/10.1109/TIM.2022.3210935.

Xu, J., Ma, X., Logsdon, S.D., Horton, R., 2012. Short, multineedle frequency domain reflectometry sensor suitable for measuring soil water content. Soil Sci. Am. J. 76, 1929–1937. http://dx.doi.org/10.2136/SSSAJ2011.0361, URL: https://onlinelibrary.wiley.com/doi/full/10.2136/sssaj2011.0361https://onlinelibrary.wiley.com/doi/abs/10.2136/sssaj2011.0361https://acsess.onlinelibrary.wiley.com/doi/10.2136/sssaj2011.0361.

Xu, Z., Zhou, W., Zhang, H., Shen, M., Liu, Y., Cai, D., Li, Y., Lei, Y., Wang, G., Bagtzoglou, A.C., Li, B., 2018. Flat thin mm-sized soil moisture sensor (MSMS) fabricated by gold compact discs etching for real-time in situ profiling. Sensors Actuators B: Chem. 255, 1166–1172. http://dx.doi.org/10.1016/j.snb.2017.05.154, URL: https://linkinghub.elsevier.com/retrieve/pii/S0925400517309772.

Yu, L., Tao, S., Ren, Y., Gao, W., Liu, X., Hu, Y., Shamshiri, R.R., 2021. Comprehensive evaluation of soil moisture sensing technology applications based on analytic hierarchy process and delphi. Agriculture 11, 1116. http://dx.doi.org/10.3390/AGRICULTURE11111116, URL: https://www.mdpi.com/2077-0472/11/11/1116/htmhttps://www.mdpi.com/2077-0472/11/11/1116, 2021 11, Page 1116.

Zambrano, C.E., Drnevich, V.P., Yu, X., Nowack, R., 2007. Soil texture from TDR waveform analysis. Symp. Appl. Geophys. Eng. Environ. Probl. 1, 108–128. http://dx.doi.org/10.4133/1.2924626, URL: https://library.seg.org/doi/10.4133/1.2924626.

Zawilski, B.M., Granouillac, F., Claverie, N., Lemaire, B., Brut, A., Tallec, T., 2022. Calculation of soil water content using dielectric permittivity measurements; benefits of soil-specific calibration. Geosci. Instrum. Methods Data Syst. http://dx.doi.org/10.5194/gi-2022-8.

Zemni, N., Bouksila, F., Slama, F., Persson, M., Berndtsson, R., Bouhlila, R., 2022. Evaluation of modified hilhorst models for pore electrical conductivity estimation using a low-cost dielectric sensor. Arab. J. Geosci. 15, 1–9. http://dx.doi.org/10.1007/S12517-022-10354-5, URL: https://link.springer.com/article/10.1007/s12517-022-10354-5, 2022 15:11.

Zhang, X., Zou, T., Lassaletta, L., Mueller, N.D., Tubiello, F.N., Lisk, M.D., Lu, C., Conant, R.T., Dorich, C.D., Gerber, J., Tian, H., Bruulsema, T., Maaz, T.M.C., Nishina, K., Bodirsky, B.L., Popp, A., Bouwman, L., Beusen, A., Chang, J., Havlík, P., Leclère, D., Canadell, J.G., Jackson, R.B., Heffer, P., Wanner, N., Zhang, W., Davidson, E.A., 2021. Quantification of global and national nitrogen budgets for crop production. Nat. Food 2, 529–540. http://dx.doi.org/10.1038/s43016-021-00318-5, URL: https://www.nature.com/articles/s43016-021-00318-5, 2021 2:7.

Zheng, C., Zhou, Q., Wang, J., Du, D., 2023. Wireless plant stresses monitoring with a wearable chemiresistor gas sensor at room temperature. Sensors Actuators B: Chem. 381, 133408. http://dx.doi.org/10.1016/J.SNB.2023.133408.

Zhu, J., Wang, H., Zhao, H., Lin, T., 2021. High depth resolution design of small diameter nuclear magnetic resonance logging probe based on compensating magnets for soil moisture measurement in situ. J. Hydrol. 603, 127031. http://dx.doi.org/10.1016/J.JHYDROL.2021.127031.